GL-TR-90-0284

A Technique for Estimating Surface Meteorological Ranges Over Oceans From Satellite Measurements of Aerosol Optical Depth

David R. Longtin
Eric P. Shettle
John R. Hummel

SPARTA, Inc.
24 Hartwell Avenue
Lexington, MA 02173

16 October 1990

Scientific Report No. 5

GEOPHYSICS LABORATORY
AIR FORCE SYSTEMS COMMAND
UNITED STATES AIR FORCE
HANSCOM AIR FORCE BASE, MASSACHUSETTS 01731-5000

"This technical report has been reviewed and approved for publication"

(Signature)
Robert R. Beland
Contract Manager

(Signature)
Donald E. Bedo, Chief
Electro-Optical Measurements Branch

FOR THE COMMANDER

(Signature)
R. Earl Good, SES, Director
Optical Environment Division

This report has been reviewed by the ESD Public Affairs Office (PA) and is releasable to the National Technical Information Service (NTIS).

Qualified requestors may obtain additional copies from the Defense Technical Information Center. All others should apply to the National Technical Information Service.

If your address has changed, or if you wish to be removed from the mailing list, or if the addressee is no longer employed by your organization, please notify GP/IMA, Hanscom AFB, MA 01731. This will assist us in maintaining a current mailing list.

Do not return copies of this report unless contractual obligations or notices on a specific document requires that it be returned.

UNCLASSIFIED

SECURITY CLASSIFICATION OF THIS PAGE

REPORT DOCUMENTATION PAGE

1a. REPORT SECURITY CLASSIFICATION UNCLASSIFIED	1b. RESTRICTIVE MARKINGS
2a. SECURITY CLASSIFICATION AUTHORITY	3. DISTRIBUTION / AVAILABILITY OF REPORT APPROVED FOR PUBLIC RELEASE; DISTRIBUTION UNLIMITED
2b. DECLASSIFICATION / DOWNGRADING SCHEDULE	
4. PERFORMING ORGANIZATION REPORT NUMBER(S) LTR90-010	5. MONITORING ORGANIZATION REPORT NUMBER(S) GL-TR-90-0284
6a. NAME OF PERFORMING ORGANIZATION SPARTA, INC. — 6b. OFFICE SYMBOL (If applicable)	7a. NAME OF MONITORING ORGANIZATION GEOPHYSICS LABORATORY
6c. ADDRESS (City, State, and Zip Code) 24 HARTWELL AVENUE LEXINGTON, MA 02173	7b. ADDRESS (City, State, and Zip Code) HANSCOM AFB, MA 01731-5000
8a. NAME OF FUNDING / SPONSORING ORGANIZATION GEOPHYSICS LABORATORY — 8b. OFFICE SYMBOL (If applicable) GL/OPA	9. PROCUREMENT INSTRUMENT IDENTIFICATION NUMBER F19628-88-C-0038
8c. ADDRESS (City, State, and Zip Code) HANSCOM AFB MA 01731-5000	10. SOURCE OF FUNDING NUMBERS

PROGRAM ELEMENT NO.	PROJECT NO.	TASK NO.	WORK UNIT ACCESSION NO.
62101F	7670	15	AP

11. TITLE (Include Security Classification,
A Technique for Estimating Surface Meteorological Ranges Over Oceans From Satellite Measurements of Aerosol Optical Depth

12. PERSONAL AUTHOR(S)
David R. Longtin, Eric P. Shettle*, and John R. Hummel

13. TYPE OF REPORT	13b. TIME COVERED	14. DATE OF REPORT (Year, Month, Day)	15. PAGE COUNT
SCIENTIFIC NO. 5	FROM 08/01/89 TO 10/01/90	16 OCTOBER 1990	66

16. SUPPLEMENTARY NOTATION
* Now at Naval Research Laboratory, Code 6522, Washington, DC 20375

17. COSATI CODES			18. SUBJECT TERMS (Continue on reverse if necessary and identify by block number)
FIELD	GROUP	SUB-GROUP	Key Words: NOAA/AVHRR data, Meteorological Range, Aerosol optical depth, aerosol profiles, SAGE comparisons

19. ABSTRACT (Continue on reverse if necessary and identify by block number)

Measurements of aerosol optical depth from NOAA Advanced Very High Resolution Radiometers (AVHRR) aboard polar-orbiting satellites have been used to estimate the surface meteorological range over oceans. To do this, a lookup table of optical depth versus meterological range has been developed which is based on the aerosol extinction profiles in LOWTRAN 7. To better simulate conditions over oceans, the boundary layer height has been lowered to 0.5 km and an extinction profile corresponding to a 150 km meteorological range has been added.

The lookup table has been applied to AVHRR aerosol optical depths near selected island locations where, in tuen, the inferred meteorological ranges were validated against surface observations. REsults show reasonable success in locating regions where meteorological ranges exceed 30 km, but more precise classification may not be possible due to uncertainties in both the measurements and observations. The algorithm tends to produce higher than observed meteorological ranges, when the observed values are less than 30 kilometers. Limited comparisons with SAGE II data, suggest that the assumed model aerosol extinction profiles, used by the algorithm may contain too much aerosol loading above the boundary layer, which could account for some, but not all, of this discrepancy. Other explanations include the possiblity the island sites have lower visibilities than the surrounding open ocean or the AVHRR optical depths are too small.

20. DISTRIBUTION / AVAILABILITY OF ABSTRACT	21. ABSTRACT SECURITY CLASSIFICATION
☐ UNCLASSIFIED/UNLIMITED ☒ SAME AS RPT. ☐ DTIC USERS	UNCLASSIFIED

22a. NAME OF RESPONSIBLE INDIVIDUAL	22b. TELEPHONE (Include Area Code)	22c. OFFICE SYMBOL
ROBERT BELAND		GL/OPA

DD FORM 1473, 84 MAR — 83 APR edition may be used until exhausted. All other editions are obsolete.

SECURITY CLASSIFICATION OF THIS PAGE
UNCLASSIFIED

Contents

Illustrations

Tables

Acknowledgement

We wish to thank Capt. Julie Hall of ESD/WE and Mr. Tomlinson of USAFETAC for their assistance in obtaining the AVHRR data. We would like to thank M.P. McCormick of NASA Langley Research Center and the SAGE II Science Team for providing the SAGE II data tapes.

A Technique for Estimating Surface Meteorological Ranges Over Oceans From Satellite Measurements of Aerosol Optical Depth

1. INTRODUCTION

Remote sensing of the atmosphere with satellite-based instrumentation is particularly useful for oceanic regions where surface observations are scarce. Atmospheric variables often monitored with satellites include temperature, moisture, aerosol profiles, and trace gas amounts. These satellite-derived data can enhance short-term weather forecasting plus they can be used for climate modeling and military applications.

Of interest to this paper are the aerosol optical depth data derived from measurements by the Advanced Very High Resolution Radiometer (AVHRR) aboard NOAA polar orbiting satellites. Specifically, AVHRR aerosol optical depths will be used to obtain information about surface meteorological ranges over oceans.

1.1 Organization of the Report

For reference, a brief description of the AVHRR aerosol data is given in Chapter 2. Our approach for estimating surface meteorological ranges from aerosol optical depths is then presented in Chapter 3. Next, our approach is applied to measured aerosol optical depth data near selected island locations, as described in Chapter 4. In Chapter 5, inferred meteorological ranges are validated against surface observations at the selected island locations. Chapter 5 also addresses the possible sources of error in our approach. Finally, Chapter 6 contains our conclusions plus recommendations for future research.

2. DESCRIPTION OF THE AVHRR AEROSOL DATA

2.1 General Information

The AVHRR instrument is mounted aboard NOAA near-polar, sun-synchronous orbiting satellites. The orbital period of the satellites is about 102 minutes which produces 14.1 orbits per day. Aerosol optical depths are derived from measurements taken when the satellites cross the equator close to local solar noon. Recently, the NOAA-9 and NOAA-11 satellites have been used to obtain aerosol optical depth data. The NOAA-11 satellite replaced the NOAA-9 satellite on November 8, 1988. The NOAA-11 satellite has provided improved global coverage because it crosses the equator around 13:30 local time (as compared with 14:30-16:30 local time for NOAA-9), allowing the AVHRR instrument to view more of the Earth with better solar illumination. The observations were limited to open oceans, where the contribution from surface reflections is small and less variable than over land. They were further restricted to at least 25 km from the continental coast lines to minimize the effects of reflections from the ocean floor. Also, to avoid problems with sun glint, only the observations in the half of the scan away from the sun are used.

The AVHRR instrument is a cross-track scanning system that measures upwelling radiation in four or five (depending on the satellite) visible and IR spectral channels.[1] The instantaneous field of view is about 1.4 milliradians in each channel leading to a resolution at the satellite subpoint of 1.1 km for a nominal altitude of 833 km. The sampling rate of the instrument gives 2048 samples per channel per Earth scan which spans an angle of $\pm 55.4^{\circ}$ from the nadir.

NOAA researchers have developed a lookup table that relates the radiance measurements from the AVHRR instrument to aerosol optical depths. Effectively, the retrieval algorithm correlates optical depths with the radiance from the upwelling Channel 1 (0.58-0.68 μm) as described by Rao *et al.*[2] and Griggs and Stowe.[3] The retrieval algorithm filters out regions containing clouds based on radiances from Channel 3 (3.55-3.93 μm). The reported optical depths have been scaled to a wavelength of 0.50 μm. The nominal accuracy of the optical depth data is ± 0.05.

---

[1] NOAA/NESDIS (1986) *NOAA Polar Orbiter Data (TIROS-N, NOAA-6, NOAA-7, NOAA-8, NOAA - 9, and NOAA-10) Users Guide*, Compiled and Edited by K. B. Kidwell (Revised January 1988), National Climatic Data Center Satellite Data Services Division, Washington, D.C.

[2] Rao, C.R.N., Stowe, L.L., McClain, E.P., and Sapper, J. (1988) Development and Application of Aerosol Remote Sensing with AVHRR Data from the NOAA Satellites, in *Aerosols and Climate*, Hobbs, P. and McCormick, M.P. (Eds.), A. Deepak Publishing, Hampton, VA, 69-79.

[3] Griggs, M. and Stowe, L.L. (1984) Measurements of Aerosol Optical Parameters from Satellites, *IRS' 84: Current Problems in Atmospheric Radiation*, G. Fiocco (Ed.), A. Deepak Publishing, Hampton, VA, 42-45.

2.2 Data Format

Global sets of total aerosol optical depth data over oceans have been made available through the NOAA National Environmental Satellite, Data and Information Service (NOAA/NESDIS). The product includes weekly contour maps of average aerosol optical depths plus archived aerosol optical depths on magnetic tapes. Each archived tape contains two files: A Header File, and an Aerosol Observation File where the latter contains all aerosol optical depth data for an eight day period.

Briefly, the organization of the Aerosol Observation File follows that of the Eight Day Sea Surface Temperature (SST) File which is a standard NOAA/NESDIS product.[1] The earth is divided into 5° by 5° blocks which are further divided into twenty five 1° by 1° subblocks. The blocks are numbered from 1 to 2592 with the first block located at 180° W and 90° S. Block numbers increase by 1 to the east and by 72 to the north. Figure 1 shows the block numbering scheme pictorially. To extract the aerosol optical depths near a particular latitude and longitude, the user must first determine the block and subblock number for the desired latitude and longitude. The first record of the Aerosol Observation File, called the directory record, then indicates where aerosol optical depths for the desired block and subblock are stored within the Aerosol Observation File. For reference, a full description of the Header File and the Aerosol Observation File is given in Appendix A.

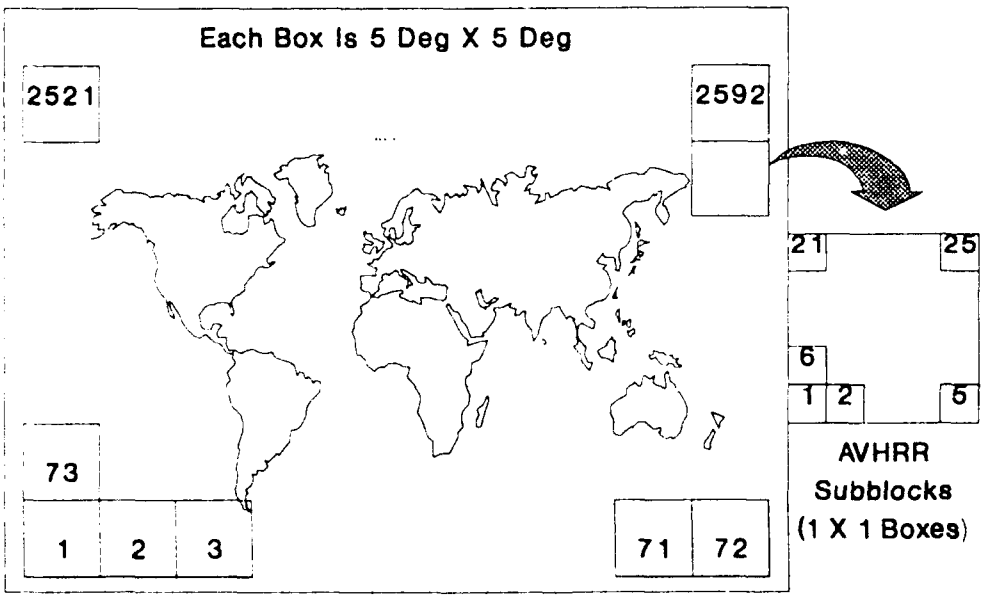

Figure 1. Block and Subblock Numbering Scheme Used to Coordinate the AVHRR Aerosol Data

3. ALGORITHM FOR INFERRING METEOROLOGICAL RANGES

The aerosol optical depth, τ, from ground to space is given by

$$\tau(\lambda) = \int_0^\infty \beta(z, \lambda) \mathrm{d}z \tag{1}$$

where β is the aerosol extinction coefficient at a wavelength λ and z is altitude. For purposes of numerical integration, Eq. 1 can be expressed as

$$\tau(\lambda) = \sum_{i=1}^{b} \beta(z_i, \lambda)\Delta z + \sum_{i=b+1}^{n} \beta(z_i, \lambda)\Delta z \tag{2}$$

where z_b is the boundary layer height. Additionally, Koschmeiders Law relates the surface meteorological range, V^*, to the surface aerosol extinction coefficient at 0.55 μm according to

$$V^* = 3.912/(\beta(z_1, 0.55) + R) \tag{3}$$

where R is the surface Rayleigh scattering coefficient at 0.55 μm and z_1 is at the surface.

The present approach assumes that aerosol contributions above the boundary layer remains fixed so that all spatial and temporal variations in total aerosol optical depth originate from the boundary layer. An independent estimate of the boundary layer height, z_b, can be used in Eq. 2, assuming that the aerosol is uniformly mixed within the boundary layer and an appropriate model aerosol extinction profile is used above the boundary layer. Lacking such an estimate, a default boundary layer thickness is used with model profiles based on those from Shettle and Fenn.[4] Next, the profiles are used in combination with Eqs. 2 and 3 to develop a lookup table of τ versus V^*. Inferred meteorological ranges are then obtained by comparing the measured values of τ with the reference values of τ and V^*. A linear interpolation in $1/\tau$ versus V^* is performed when a measured value of τ is between reference values.

The original Shettle and Fenn profiles while based on a large number of data sources, were derived almost exclusively from measurements over land. Because of this, their aerosol extinction profiles have been modified in several ways to

[4] Shettle, E.P. and Fenn, R.W. (1976) Models of the Atmospheric Aerosols and Their Optical Properties, in AGARD Conference Proceedings No. 183 *Optical Propagation in the Atmosphere* presented at the Electromagnetic Wave Propagation Panel Symposium, Lyngby, Denmark, 27-31 October 1975, AGARD-CP-183, (AD A028-615).

better simulate conditions over oceans. The height of the boundary layer was reduced to 0.5 km which represents a generic ocean boundary layer height as reported by Oke[5] and supported by the measurements of Gathman *et al.*[6] Also an extinction profile for a meteorological range of 150 km was added to original Shettle and Fenn model as a way of accounting for a very clean atmosphere. Furthermore, aerosol extinction between the altitudes of 1 and 5 km was modeled using the profile for the 150 km meteorological range. Except for oceanic regions with strong continental influence, this approach is suitable for the free troposphere over oceans because cloud processes continuously remove aerosols and because maritime aerosol production is usually confined to the boundary layer. Finally, appropriate wavelength scaling factors have been applied to the Shettle and Fenn data because meteorological range is defined at 0.55 μm and the AVHRR data are for 0.50 μm, respectively.

For reference, Table 1 lists the adopted aerosol extinction profiles for Fall/Winter and Spring/Summer conditions. Figure 2 shows these values pictorially. The original Shettle and Fenn[4] aerosol profiles were used for the free troposphere and their background stratospheric model was used above the tropopause. (Tabulated values for these aerosol profiles are given by Fenn et al.[7]) The resulting reference values of τ versus V^* are listed in Table 2 and shown in Figure 3.

---

[5] Oke, T.R. (1978) *Boundary Layer Climates*, Methuen Publishing, New York, 89-90.

[6] Gathman, S.G, de Leeuw, G., Davidson, K.L., and Jensen, D.R. (1979) The Naval Oceanic Vertical Aerosol Model: Progress Report, in AGARD Conference Proceedings *Atmospheric Propagation in the UV, Visible, IR and MM-Wave Region and Related System Aspects*, presented at 45th Symposium Electromagnetic Wave Propagation Panel, Copenhagen Denmark, 9-13 October 1989.

[7] Fenn, R.W., Clough, S.A., Gallery, W.O., Good, R.E., Kneizys, F.X., Mill, J.D., Rothman, L.S., Shettle, E.P., and Volz, F.E. (1985) Optical and Infrared Properties of the Atmosphere, Chapter 18 in *Handbook of Geophysics and the Space Environment*, A.S. Jursa Scientific Ed., Air Force Geophysics Laboratory, Hanscom AFB, MA, AFGL-TR-85-0315, (AD A167000).

Table 1. Adopted Aerosol Extinction Below 5 km As a Function of Meteorological Range. Aerosol extinction is at 0.55 μm and V* is in km

Aerosol Extinction (km^{-1}) for Fixed V*							
z (km)	150 FW	150 SS	50	23	10	5	2
0.0	0.0141	0.0141	0.0662	0.158	0.379	0.770	1.94
0.5	0.0127	0.0135	0.0530	0.123	0.379	0.770	1.94
1.0	0.0115	0.0130					
1.5	0.0103	0.0125	Use profiles for V* = 150 km				
2.0	0.00925	0.0120					
3.0	0.00742	0.0111					
4.0	0.00598	0.0102					
5.0	0.00485	0.00930					

FW: Fall/Winter SS: Spring/Summer

Table 2. Aerosol Optical Depth at 0.50 μm Versus Meteorological Range for Fall/Winter (FW) and Spring/Summer (SS) Conditions

V*(Km)	τ (FW)	τ (SS)
150	0.071	0.103
50	0.105	0.136
23	0.165	0.196
10	0.353	0.384
5	0.655	0.686
2	1.557	1.588

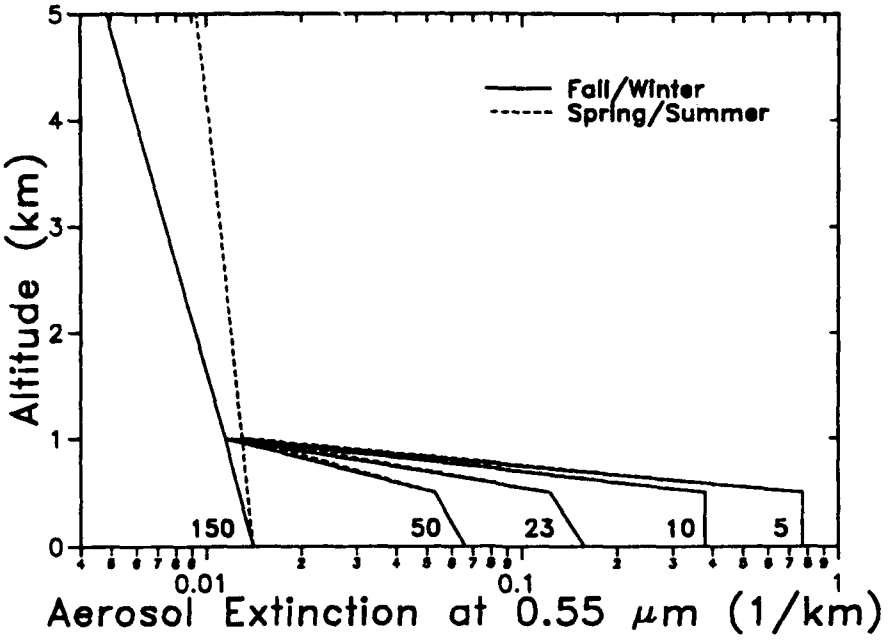

Figure 2. Assumed Aerosol Extinction Profiles for Fixed Surface Meteorological Ranges. The profiles are modified versions of Shettle and Fenn.[4] The profiles are for surface meteorological ranges of 150, 50, 23, 10, and 5 km

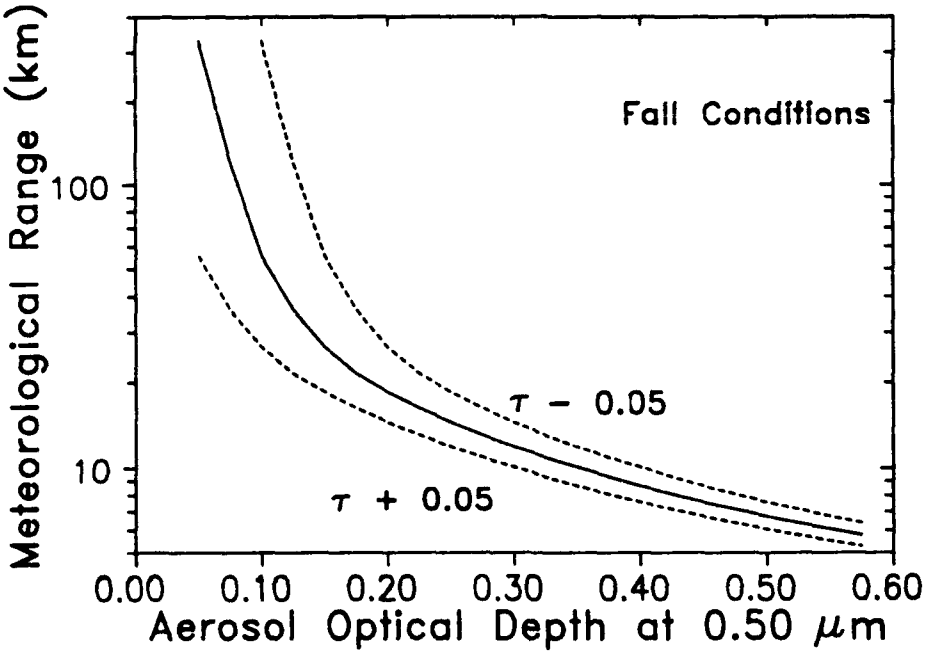

Figure 3. Calculated Aerosol Optical Depth Versus Surface Meteorological Range. Dashed lines establish a range due to uncertainties in the AVHRR measurements (±0.05)

4. VALIDATION SCHEME

4.1 Island Locations Used for Validation

Surface visibility data have been obtained for nineteen island locations from the USAFETAC DATSAV2 database network[8] (see Table 3). (This database contains all synoptic, METAR, SMARS, AMOS, AERO, MARS, and airways observations transmitted by the worldwide network of reporting stations.) The visibility data were selected to fall as close as possible to the AVHRR overpass; usually this was 1300 or 1400 local time. Occasionally, only the 1200 or 1500 observations were available.

Table 3. Island Locations For Which Surface Visibility Data Have Been Obtained

NO.	LOCATION	LAT	LONG	ETAC STATION	AVHRR BLOCK	AVHRR SUBBLOCK
1	Anderson, Guam	13.58N,	144.93E	912180	1505	20
2	Lajes, Azores	38.77N,	27.10W	085090	1831	18
3	Keflavik, Iceland	63.59N,	22.60W	040180	2192	18
4	Midway Island	28.22N,	177.37W	910660	1657	18
5	Kwajalein, Marshall Islands	8.73N,	167.73E	913660	1438	18
6	Honolulu Intl Airport, HI	21.35N,	157.93W	911820	1589	8
7	Sheyma, Aleutian Islands	52.72N,	174.12E	704140	2087	15
8	Gran Canaria, Canary Islands	27.56N,	15.38W	600300	1689	15
9	Diego Garcia	7.35S,	72.48E	619670	1203	13
10	Bermuda/Kindley	32.37N	64.68W	780160	1752	11
11	Catania/Fontanarosa, Sicily	37.47N,	15.05E	164600	1840	11
12	Block Island, RI	41.17N,	71.58W	725058	1894	9
13	Freeport Intl Airport, Bahamas	26.55N,	78.70W	780620	1677	7
14	Norman Manley/Kinos, Jamaica	17.93N,	76.78W	783970	1533	14
15	San Juan Intl Airport, PR	18.43N,	66.00W	785260	1535	20
16	Grytviken Georgia, Falkland Isl.	54.27S,	36.50W	889030	533	4
17	Tahiti Island	17.55S,	149.62W	919380	1015	11
18	Auckland Intl Airport, NZ	37.02S,	174.80E	931190	791	15
19	Ascension Island	7.97S,	14.40W	619020	1186	11

[8] USAFETAC (1986) DATSAV2 Surface Climatic Database Users Handbook No. 4, available from USAFETAC, Federal Building, Asheville, N.C.

Examination of the visibility data suggested that some island locations were not suitable for validation purposes. For example, some stations use reporting codes that limit the maximum reportable visibility and, therefore, prevent an objective and fair assessment of our algorithm. Also, some stations were located in cold ocean waters and often reported very low visibilities due to locally dense fogs which may not be representative of the surrounding ocean areas. Consequently, we have limited our study to the seven island locations shown in Figure 4. The maximum visibilities for these stations are listed in Table 4. For reference, Table 5 lists those island stations that were omitted, as well as the reasons why they were omitted.

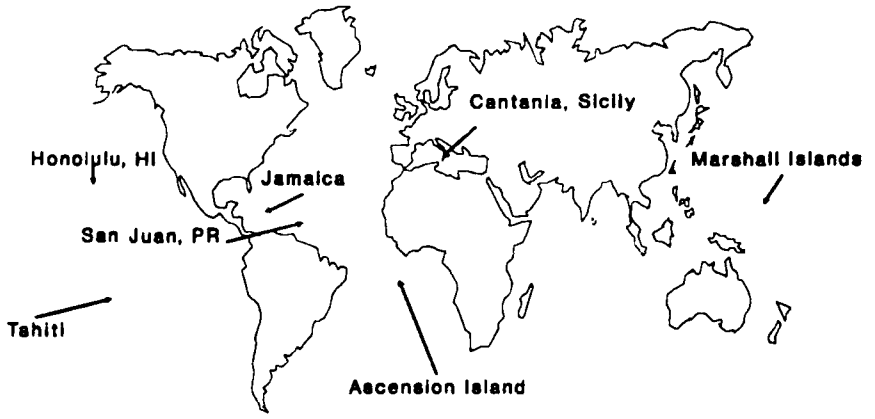

Figure 4. Island Locations Used for Validation

For days when both measured optical depths (see Section 4.2) and observed surface visibilities are available, we have corrected for the difference between surface meteorological range as defined by the Koschmeider relationship, (Eq. 3), and observed surface visibility. The correction factor is $V^* = 1.3V_{obs}$, as suggested by Gordon.[9]

[9] Gordon, J.I. (1979) "Daytime Visibility, A Conceptional Review," Air Force Geophysics Laboratory, Hanscom AFB, MA, AFGL-TR-79-0257, (AD A08544-51).

Table 4. Island Locations Used for Validation

NO.	LOCATION	MAXIMUM REPORTED VISIBILITY (KM)
5	Kwajalein, Marshall Island	24.0
6	Honolulu Intl Airport, Hawaii	40.0
11	Cantania/Fontanarosa, Sicily	30.0
14	Norman Manley/Kinos, Jamaica	30.0
15	San Juan Intl Airport, Puerto Rico	35.0
17	Tahiti Island	40.0
19	Ascension Island	75.0

Table 5. Island Locations Not Used For Validation

NO.	LOCATION	REASON
1	Anderson, Guam	Airway reports only (maximum reported visibility of 11.2 km)
2	Lajes, Azores	" "
3	Keflavik, Iceland	" "
4	Midway Island	" "
7	Sheyma, Aleutian Islands	Highly variable visibilities due to locally dense fog
8	Gran Canaria, Canary Islands	Airway reports only (maximum reported visibitity of 11.2 km)
9	Diego Garcia	" "
10	Bermuda/Kindley	" "
12	Block Island, Rhode Island	Visibilities usually not reported
13	Freeport Intl Airport, Bahamas	Maximum reported visibility below 23 km
16	Grytviken Georgia, Falkland Isl	Highly variable visibilites due to locally dense fog
18	Auckland Intl Airport, New Zealand	Infrequent reports

4.2 Optical Depth Data Reduction

Average optical depths were computed for each day that observations occurred near a given island location. For an observation to be included in the average for an island location, it had to fall within the $5° \times 5°$ AVHRR block defining that island location. Furthermore, the relative variability was also calculated to keep track of variability within each $5° \times 5°$ block of observations. (Relative variability is defined as $\sigma/\overline{\tau}$ where σ and $\overline{\tau}$ are the standard deviation and average, respectively, for a $5° \times 5°$ block.) Those average optical depths having excessive variability were subsequently removed because they would not fairly represent the observed visibilities at island locations. To be included in our validation scheme, an average optical depth must have a relative variability ≤ 0.33 or $2\sigma \leq 0.05$. Figure 5 shows a scatter plot of relative variability versus average optical depth using all available data near the seven island locations. As expected, relative variabilities are largest when $\overline{\tau} \leq 0.05$ because $\overline{\tau}$ is less in magnitude than the nominal accuracy (± 0.05) of the AVHRR product. Many of these average optical depths are retained for validation, however, because they satisfy the criterion of $2\sigma \leq 0.05$.

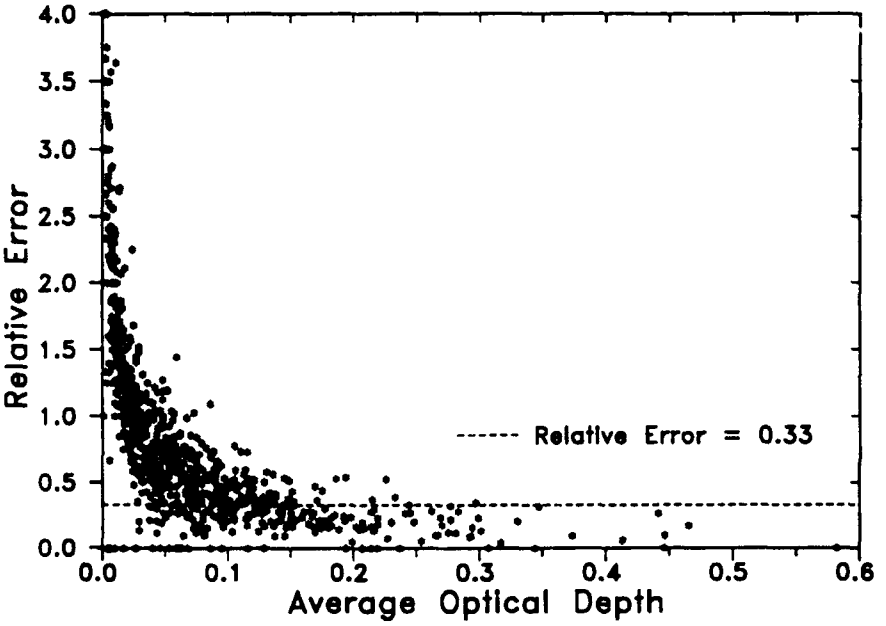

Figure 5. Relativity Variability Versus Average Optical Data. Scatter plot includes all available data near the island locations for October 1988 and June 1989 to February 1990. Relative variability equals $\sigma/\overline{\tau}$ where $\overline{\tau}$ is the average optical depth and σ is the standard deviation

4.3 File Processing Details

The eight day AVHRR Aerosol Observation Files for October 1988 and June 1989-February 1990 were read and copied onto GL computer center tapes. Additionally, optical depth data near the nineteen island locations were extracted from the original Aerosol Observation Files and copied onto GL computer center RECLAIM tapes. These "extracted" files contain all optical depth data that fall within an AVHRR block defining an island location, or one of its eight adjacent blocks ($15^\circ \times 15^\circ$ in all). For reference, a description of the computer programs used to process the AVHRR data is given in Appendix B. Also the GL computer tapes and their contents are listed in Appendix B.

5. INFERRED AND OBSERVED METEOROLOGICAL RANGES

5.1 Method of Comparison

As a first approach, we constructed a frequency distribution table showing the number of times the inferred meteorological ranges agreed with their corresponding observed values. In developing the table, the data were grouped into range bins of <10, 10-20, 20-30 and >30 km. Here the amount of agreement is measured by the number of times when inferred ranges fell within the same range bin as the observed values. The results were convienently expressed as histograms.

At this point, we should mention that only one range bin is used for data exceeding 30 km because both the inferred and observed values are subject to large errors during very clear conditions. For example, island locations often lack sufficient reference points to accurately establish the visibility during very clear conditions. Consequently, stations often report some (maximum) visibility when, in fact, the true visibility may actually exceed that value. In addition to uncertainities in the observed data, inferred meteorological ranges are extremely sensitive to small changes in $\overline{\tau}$ during very clear conditions (see Figure 3). This problem is further compounded because values of $\overline{\tau}$ are often less in magnitude than the nominal accuracy (± 0.05) of the AVHRR product.

5.2 Results

A frequency distribution table of inferred meteorological range for observed range bins is given in Table 6. Figure 6 expresses these results as histograms. (For reference, daily comparisons of inferred and observed meteorological ranges are given in Appendix C.) The histograms suggest limited success in inferring the meteorological range in regions of moderate and high aerosol loading. Of most concern is the frequency in which inferred meteorological ranges exceed 30 km when observed values are less than 20 km. Also, our algorithm has trouble with

regions where the observed values are between 20-30 km. Since the inferred meteorological ranges are generally too large, the following possible explanations are offered:

1. The assumed aerosol profiles have too much total aerosol loading for a given V^*. Adopting an exponential extinction profile in the boundary layer (in place of the step function currently used) would likely improve our results for observed ranges less than 10 km
2. The correction from V_{obs} to V^* needs to be larger, *i.e.*, $V^* = 1.6V_{obs}$
3. The AVHRR optical depths are systematically too small
4. The island sites utilized generally have lower visibilities than the surrounding open ocean water where most of the optical thickness data was derived.

Table 6. Number of Times That the Inferred Values of Meteorological Range Agreed or Disagreed with the Concurrently Observed Values

	Inferred Meteorological Range (km)			
Observed	<10	10-20	20-30	>30
<10	2	7	1	17
10-20	4	10	16	56
20-30	2	5	4	70
>30	0	14	15	349

During clear conditions, on the other hand, there is better agreement between inferred and observed meteorological ranges. Therefore, our algorithm could prove useful for aerosol applications in which it is only necessary to know when the meteorological range exceeds a value representative of a clean atmosphere, say 30 km.

5.3 Comparisons Between Adopted Aerosol Profiles and Those from SAGE

In an effort to determine why the inferred and observed meteorological ranges differ, we have obtained aerosol extinction measurements from the Stratospheric Aerosol and Gas Experiment II (SAGE II). The SAGE II instrument was developed for the Earth Radiation Budget Satellite (ERBS) to monitor the global distribution of stratospheric aerosols, ozone, water vapor, and nitrogen dioxide (see Mauldin et al.[10] and McCormick et al.[11]). The vertical distributions of these species are

[10] Mauldin III, L.E., Zaun, N.H., McCormick, M.P., Guy, J.H., and Vaughn, W.R. (1985) Stratospheric Aerosol and Gas Experiment II Instrument: A Functional Description, *Opt. Engineering*, **24**: 307-312.

[11] McCormick, M.P., Hamill, P., Pepin, T.J., Chu, W.P., Swissler, T.J., and McMaster, L.R. (1979) Satellite Studies of the Stratospheric Aerosol, *Bull. Amer. Meteor. Soc.*, **60**: 1038-1046.

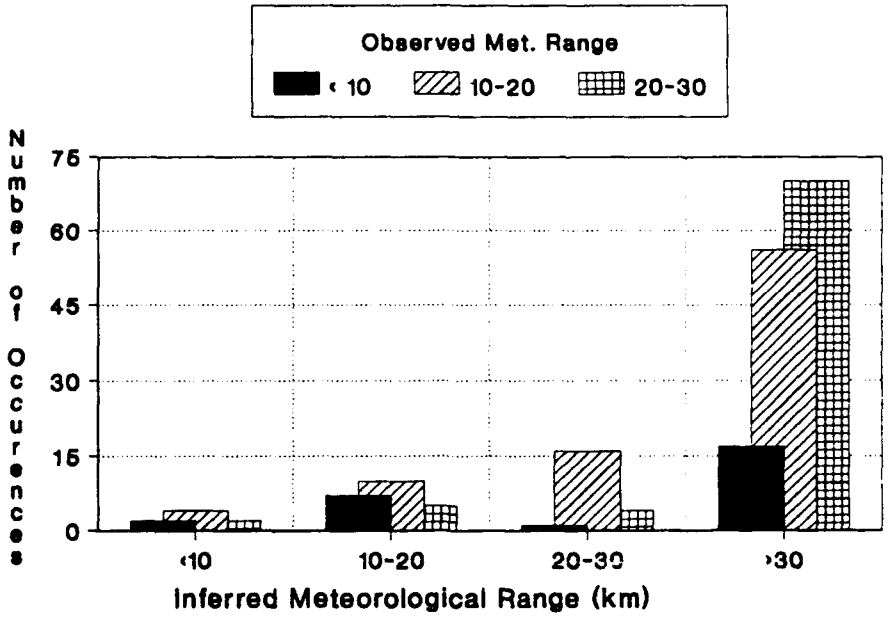

(a)

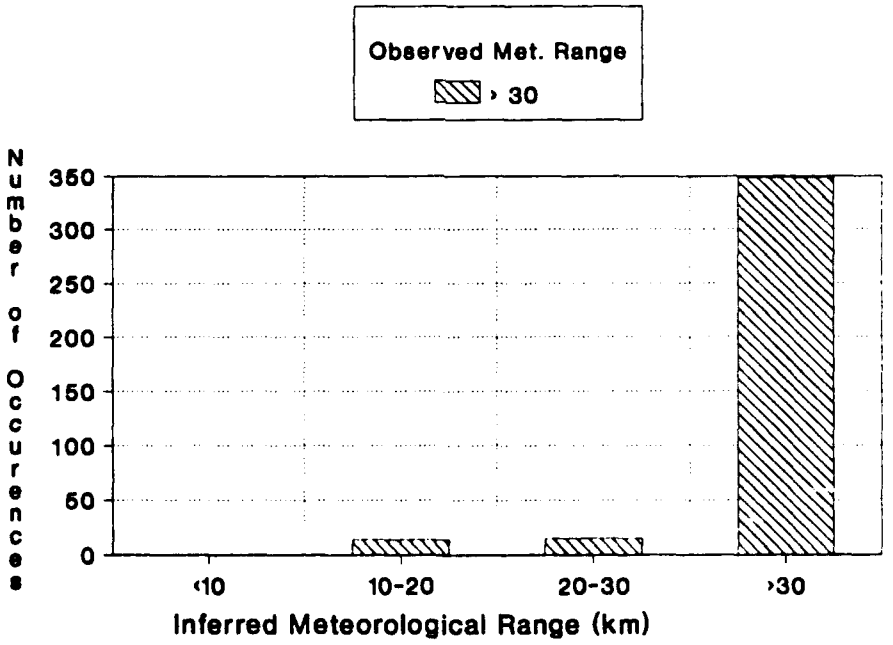

(b)

Figure 6. Histogram Showing the Agreement Between Values of Inferred and Observed Meteorological Range (a) for Observed Values <10, 10-20, and 20-30 km (b) for Observed Values >30 km. For example, the leftmost solid bar in Figure 6(a) indicates that on two occasions, inferred meteorological ranges were less than 10 km and observed values were also less than 10 km

determined from measurements of solar extinction through the earth's atmospheric limb, at seven spectral wavelengths during ERBS observatory occultations. Four of these wavelengths provide aerosol attenuation data (0.385, 0.452, 0.525, and 1.02 μm). Validation of the SAGE II aerosol measurements along with some initial data analysis is given in a special issue of the *Journal of Geophysical Research* (see Russell and McCormick[12] and the accompanying nine papers in that issue). While designed primarily for stratospheric measurements, the SAGE instrument can obtain tropospheric aerosol attenuation data, particularly at the longer wavelengths, for cloud-free lines of sight. About half of all profiles provide aerosol attenuation data down to 5 km at 1.02 μm. The spatial coverage of SAGE data includes the seven island locations used for validation purposes.

We extracted SAGE aerosol profiles near the seven island locations for the Fall 1988 and Summer 1989 time periods. For a profile to be considered near an island, it had to be within 5 degrees of the island. These aerosol extinction profiles were then integrated to obtain aerosol optical depths at 0.525 and 1.02 μm. For each profile, two aerosol optical depths were computed. The first optical depth was for the region above 10 km and the second represented the full range of available data. Using our adopted aerosol profiles (see Table 1), we then computed aerosol optical depths for the same altitude regions. Here, the Fall/Winter and Spring/Summer profiles were used for comparisons with Fall 1988 and Summer 1989 SAGE data, respectively. Also, appropriate wavelength scaling factors (Shettle and Fenn[13]) were applied to the AFGL model profiles for comparisons with the SAGE data at 1.02 μm. Before comparing SAGE and model optical depths, we examined the SAGE profiles for the presence of clouds. Those profiles containing aerosol extinction greater than 0.01 1/km, suggesting the presence of clouds, were removed from the comparisons.

Tables 7 and 8 compare SAGE and model optical depths above 10 km for 0.525 and 1.02 μm, respectively. Generally there is good agreement between the SAGE and model optical depths at 0.525 μm which suggests that our adopted profiles above the troposphere are reasonable. At 1.02 μm however, the model optical depths tend to be less than those obtained from SAGE.

Tables 9 and 10 compare model optical depths against the full SAGE optical depths. For reference, the altitude ranges of the SAGE profiles are given in both tables. The results in Table 9 suggest that model aerosol optical depths above 5 km are generally greater than those from the SAGE data, especially for the most

[12] Russell, P.B. and McCormick, M.P. (1989) SAGE II Aerosol Data Validation and Initial Data Use: An Introduction and Overview, *J. Geophys. Res.*, **94**: 8335-8338.

[13] Shettle, E.P. and Fenn, R.W. (1979), "Models of the Aerosols of the Lower Atmosphere and the Effects of Humidity Variations," Hanscom AFB, MA, AFGL-TR-79-0214, (AD A085615).

Table 7. Comparisons Between SAGE and Model Aerosol Optical Depths at 0.525 μm for the 10.0-45.0 km Altitude Range

LOCATION	DATE	τ_{SAGE}	τ_{AFGL}	ABSOLUTE DIFFERENCE	PERCENT DIFFERENCE
Honolulu, HI	11/2/88	9.10×10^{-3}	8.72×10^{-3}	3.81×10^{-4}	4.4
Honolulu, HI	11/3/88	8.31×10^{-3}	8.72×10^{-3}	-4.11×10^{-4}	-4.7
Cantania, Sicily	9/16/88	1.41×10^{-2}	8.72×10^{-3}	5.42×10^{-3}	62.2
Cantania, Sicily	10/9/88	7.80×10^{-3}	8.72×10^{-3}	-9.18×10^{-4}	-10.5
Cantania, Sicily	10/30/88	8.22×10^{-3}	8.72×10^{-3}	-4.93×10^{-4}	-5.7
Cantania, Sicily	11/5/88	8.47×10^{-3}	8.72×10^{-3}	-2.43×10^{-4}	-2.8
Cantania, Sicily	11/27/88	9.38×10^{-3}	8.72×10^{-3}	6.65×10^{-4}	7.6
Cantania, Sicily	11/28/88	9.42×10^{-3}	8.72×10^{-3}	7.02×10^{-4}	8.0
Cantania, Sicily	11/29/88	9.31×10^{-3}	8.72×10^{-3}	5.96×10^{-4}	6.8
Cantania, Sicily	7/2/89	7.86×10^{-3}	7.46×10^{-3}	3.98×10^{-4}	5.3
Cantania, Sicily	7/3/89	6.87×10^{-3}	8.43×10^{-3}	-1.56×10^{-3}	-18.6
Cantania, Sicily	7/26/89	5.41×10^{-3}	8.43×10^{-3}	-3.02×10^{-3}	-35.8
Cantania, Sicily	7/27/89	7.20×10^{-3}	8.43×10^{-3}	-1.24×10^{-3}	-14.6
San Juan, Puerto Rico	11/1/88	8.27×10^{-3}	8.72×10^{-3}	-4.51×10^{-4}	-5.2
San Juan, Puerto Rico	11/2/88	6.73×10^{-3}	8.72×10^{-3}	-1.98×10^{-3}	-22.8
Ascension Island	9/22/88	1.18×10^{-2}	8.72×10^{-3}	3.10×10^{-3}	35.6
Ascension Island	9/23/88	1.19×10^{-2}	8.72×10^{-3}	3.20×10^{-3}	36.8
Ascension Island	10/1/88	1.70×10^{-2}	8.72×10^{-3}	8.30×10^{-3}	95.2
Ascension Island	7/13/89	7.50×10^{-3}	8.43×10^{-3}	-9.30×10^{-4}	-11.0
Ascension Island	7/16/89	6.69×10^{-3}	8.43×10^{-3}	-1.74×10^{-3}	-20.6
Ascension Island	7/17/89	6.11×10^{-3}	8.43×10^{-3}	-2.33×10^{-3}	-27.6
Tahiti Island	7/14/89	7.24×10^{-3}	8.43×10^{-3}	-1.20×10^{-3}	-14.2
Tahiti Island	8/27/89	9.89×10^{-3}	8.43×10^{-3}	1.46×10^{-3}	17.3

Note: Sicily Profile for 7/2/89 ends at 11 km

Table 8. Comparisons Between SAGE and Model Aerosol Optical Depths at 1.02 μm for the 10.0-45.0 km Altitude Range

LOCATION	DATE	τ_{SAGE}	τ_{AFGL}	ABSOLUTE DIFFERENCE	PERCENT DIFFERENCE
Honolulu, HI	11/2/88	3.03×10^{-3}	3.33×10^{-3}	-2.98×10^{-4}	-8.9
Honolulu, HI	11/3/88	2.60×10^{-3}	3.33×10^{-3}	-7.28×10^{-4}	-21.9
Cantania, Sicily	9/16/88	4.05×10^{-3}	3.33×10^{-3}	7.21×10^{-4}	21.6
Cantania, Sicily	10/9/88	2.18×10^{-3}	3.33×10^{-3}	-1.16×10^{-3}	-34.7
Cantania, Sicily	10/30/88	2.50×10^{-3}	3.33×10^{-3}	-8.34×10^{-4}	-25.0
Cantania, Sicily	11/5/88	2.42×10^{-3}	3.33×10^{-3}	-9.12×10^{-4}	-27.4
Cantania, Sicily	11/27/88	2.51×10^{-3}	3.33×10^{-3}	-8.27×10^{-4}	-24.8
Cantania, Sicily	11/28/88	2.71×10^{-3}	3.33×10^{-3}	-6.22×10^{-4}	-18.7
Cantania, Sicily	11/29/88	2.58×10^{-3}	3.33×10^{-3}	-7.49×10^{-4}	-22.5
Cantania, Sicily	7/2/89	2.09×10^{-3}	2.90×10^{-3}	-8.12×10^{-4}	-28.0
Cantania, Sicily	7/3/89	2.05×10^{-3}	3.23×10^{-3}	-1.19×10^{-3}	-36.7
Cantania, Sicily	7/26/89	1.76×10^{-3}	3.23×10^{-3}	-1.47×10^{-3}	-45.5
Cantania, Sicily	7/27/89	2.11×10^{-3}	3.23×10^{-3}	-1.12×10^{-3}	-34.8
San Juan, Puerto Rico	11/1/88	2.83×10^{-3}	3.33×10^{-3}	-5.07×10^{-4}	-15.2
San Juan, Puerto Rico	11/2/88	2.51×10^{-3}	3.33×10^{-3}	-8.22×10^{-4}	-24.7
Ascension Island	9/22/88	4.45×10^{-3}	3.33×10^{-3}	1.12×10^{-3}	33.5
Ascension Island	9/23/88	3.95×10^{-3}	3.33×10^{-3}	6.17×10^{-4}	18.5
Ascension Island	10/1/88	5.39×10^{-3}	3.33×10^{-3}	2.06×10^{-3}	61.9
Ascension Island	7/13/89	2.62×10^{-3}	3.23×10^{-3}	-6.19×10^{-4}	-19.1
Ascension Island	7/16/89	2.52×10^{-3}	3.23×10^{-3}	-7.11×10^{-4}	-22.0
Ascension Island	7/17/89	2.47×10^{-3}	3.23×10^{-3}	-7.62×10^{-4}	-23.6
Tahiti Island	7/14/89	2.55×10^{-3}	3.23×10^{-3}	-6.87×10^{-4}	-21.3
Tahiti Island	8/27/89	3.28×10^{-3}	3.23×10^{-3}	4.68×10^{-5}	1.4

Note: Sicily Profile for 7/2/89 ends at 11 km

remote island locations. When these results are considered along with Table 7 for 0.525 μm, it is clear that the model profiles contain too much aerosol loading in the upper troposphere (between 5 and 10 km). Interestingly, the comparisons for Cantania, Sicily sometimes show better agreement possibly because this island can be influenced by the continental aerosols from Europe during certain synoptic conditions. However, the general differences between the SAGE and model profiles could be important when put in the context of our inferred and observed meteorological ranges. That is, replacing our assumed profiles above 5 km with SAGE profiles will likely lead to better agreement between inferred and observed meteorological ranges. It is difficult to draw clear conclusions from Table 10 given the wide range of percent errors (-81.6 to 434.8). However, the wide range of percent errors, by themselves, may indicate more aerosol variability between 1.5 and 5 km than previously expected over oceans.

An effort was made to look at those cases where tropospheric aerosol profiles from SAGE were available in the same 5° by 5° block as the AVHRR optical depths on the same day. (There is generally a several hour difference between the two, since the AVHRR data are taken near 1330 local time, and the SAGE measurements at sunrise or sunset.) In this analysis, only the blocks containing the seven island locations were considered. There were only three such cases, plus two other cases with the SAGE measurements made on the preceding day, and one case, two days following (see Table 11). The SAGE optical thickness values, τ_{SAGE}, represent the 0.525 μm wavelength, down to an altitude of H_{min}. The optical thicknesses based on the model profiles (*i.e.*, Shettle and Fenn[4]) down to the same altitude are indicated by τ_{model}. For this analysis, the ratio of the SAGE and model optical thicknesses was then used to scale model optical thicknesses above 1 km. Eq. 1 then becomes

$$\tau(\lambda) = \int_0^{1km} \beta(z,\lambda)\mathrm{d}z + \frac{\tau_{SAGE}}{\tau_{model}} \int_{1km}^{\infty} \beta(z,\lambda)\mathrm{d}z \qquad (4)$$

Effectively, Eq. 4 leads to a modified version of Table 2 and Figure 3, for optical thickness as a function of surface meteorological range. The resulting values of the SAGE corrected meteorological range, V_{cor}, are shown in the last column of Table 11. For reference, the meteorological range inferred by the original algorithm, V_{inf}, and the observed value, V_{obs}, are also shown.

In all cases, the SAGE optical depth was less than the model value and, except for the Ascension 10/3/88 case, improved the inferred meteorological range. In this last case, the difference between the observed and inferred meteorological range can be explained by an error of 0.02 in the AVHRR optical depth, which is

Table 9. Comparisons Between SAGE and Model Aerosol Optical Depths at 0.525 μm for the Full Altitude Range of SAGE Data

LOCATION	DATE	RANGE OF SAGE (km)	τ_{SAGE}	τ_{AFGL}	ABSOLUTE DIFFERENCE	PERCENT DIFFERENCE
Honolulu, HI	11/2/88	4.5-45.0	9.24×10^{-3}	2.52×10^{-2}	-1.59×10^{-2}	-63.3
Honolulu, HI	11/3/88	4.5-45.0	9.80×10^{-3}	2.52×10^{-2}	-1.54×10^{-2}	-61.1
Cantania, Sicily	10/9/88	4.5-45.0	9.80×10^{-3}	2.52×10^{-2}	-1.54×10^{-2}	-61.1
Cantania, Sicily	10/30/88	7.5-45.0	1.06×10^{-2}	1.26×10^{-2}	-2.04×10^{-3}	-16.1
Cantania, Sicily	11/5/88	5.5-45.0	2.94×10^{-2}	1.98×10^{-2}	9.68×10^{-3}	49.0
Cantania, Sicily	11/27/88	4.5-45.0	2.89×10^{-2}	2.52×10^{-2}	3.73×10^{-3}	14.8
Cantania, Sicily	11/28/88	4.5-45.0	1.14×10^{-2}	2.52×10^{-2}	-1.37×10^{-2}	-54.6
Cantania, Sicily	11/29/88	5.5-45.0	2.16×10^{-2}	1.98×10^{-2}	1.80×10^{-3}	9.1
Cantania, Sicily	7/2/89	11.5-45.0	7.86×10^{-3}	7.46×10^{-3}	3.98×10^{-4}	5.3
Cantania, Sicily	7/3/89	4.5-45.0	1.02×10^{-2}	4.25×10^{-2}	-3.23×10^{-2}	-75.9
Cantania, Sicily	7/26/89	5.5-45.0	8.86×10^{-3}	3.28×10^{-2}	-2.39×10^{-2}	-72.9
Cantania, Sicily	7/27/89	5.5-45.0	9.51×10^{-3}	3.28×10^{-2}	-2.32×10^{-2}	-71.0
San Juan, Puerto Rico	11/1/88	4.5-45.0	1.31×10^{-2}	2.52×10^{-2}	-1.21×10^{-2}	-48.1
San Juan, Puerto Rico	11/2/88	4.5-45.0	7.05×10^{-3}	2.52×10^{-2}	-1.81×10^{-2}	-72.0
Ascension Island	9/22/88	4.5-45.0	1.41×10^{-2}	2.52×10^{-2}	-1.11×10^{-2}	-44.0
Ascension Island	9/23/88	4.5-45.0	1.54×10^{-2}	2.52×10^{-2}	-9.75×10^{-3}	-38.7
Ascension Island	10/1/88	4.5-45.0	2.07×10^{-2}	2.52×10^{-2}	-4.50×10^{-3}	-17.9
Ascension Island	7/12/89	4.5-45.0	2.67×10^{-2}	4.25×10^{-2}	-1.58×10^{-2}	-37.1
Ascension Island	7/13/89	4.5-45.0	7.98×10^{-3}	4.25×10^{-2}	-3.45×10^{-2}	-81.2
Ascension Island	7/16/89	4.5-45.0	7.05×10^{-3}	4.25×10^{-2}	-3.55×10^{-2}	-83.4
Ascension Island	7/17/89	4.5-45.0	6.68×10^{-3}	4.25×10^{-2}	-3.58×10^{-2}	-84.3
Tahiti Island	7/14/89	6.5-45.0	9.09×10^{-3}	2.42×10^{-2}	-1.52×10^{-2}	-62.5
Tahiti Island	8/27/89	4.5-45.0	1.10×10^{-2}	4.25×10^{-2}	-3.15×10^{-2}	-74.1

Table 10. Comparisons Between SAGE and Model Aerosol Optical Depths at 1.02 μm for the Full Altitude Range of SAGE Data

LOCATION	DATE	RANGE OF SAGE (km)	τ_{SAGE}	τ_{AFGL}	ABSOLUTE DIFFERENCE	PERCENT DIFFERENCE
Honolulu, HI	11/2/88	0.0-45.0	4.46×10^{-2}	2.97×10^{-2}	1.49×10^{-2}	50.0
Honolulu, HI	11/3/88	0.5-45.0	3.90×10^{-2}	2.38×10^{-2}	1.52×10^{-2}	63.8
Cantania, Sicily	10/9/88	1.5-45.0	1.23×10^{-2}	1.99×10^{-2}	-7.54×10^{-3}	-38.0
Cantania, Sicily	10/30/88	7.5-45.0	4.83×10^{-3}	4.87×10^{-3}	-3.66×10^{-5}	-0.8
Cantania, Sicily	11/5/88	5.5-45.0	4.11×10^{-2}	7.68×10^{-3}	3.34×10^{-2}	434.8
Cantania, Sicily	11/27/88	3.5-45.0	5.56×10^{-2}	1.25×10^{-2}	4.31×10^{-2}	345.6
Cantania, Sicily	11/28/88	2.5-45.0	3.85×10^{-2}	1.58×10^{-2}	2.28×10^{-2}	144.5
Cantania, Sicily	11/29/88	5.5-45.0	1.30×10^{-2}	7.68×10^{-3}	5.36×10^{-3}	69.8
Cantania, Sicily	7/2/89	11.5-45.0	2.09×10^{-3}	2.90×10^{-3}	-8.12×10^{-4}	-28.0
Cantania, Sicily	7/3/89	2.5-45.0	3.46×10^{-2}	2.55×10^{-2}	9.16×10^{-3}	36.0
Cantania, Sicily	7/26/89	5.5-45.0	5.32×10^{-3}	1.28×10^{-2}	-7.51×10^{-3}	-58.5
Cantania, Sicily	7/27/89	5.5-45.0	4.35×10^{-3}	1.28×10^{-2}	-8.48×10^{-3}	-66.1
San Juan, Puerto Rico	11/1/88	2.5-45.0	3.00×10^{-2}	1.58×10^{-2}	1.42×10^{-2}	90.2
San Juan, Puerto Rico	11/2/88	2.5-45.0	1.99×10^{-2}	1.58×10^{-2}	4.16×10^{-3}	26.4
Ascension Island	9/22/88	3.5-45.0	5.31×10^{-2}	1.25×10^{-2}	4.06×10^{-2}	325.8
Ascension Island	9/23/88	2.5-45.0	2.72×10^{-2}	1.58×10^{-2}	1.14×10^{-2}	72.3
Ascension Island	10/1/88	2.5-45.0	6.26×10^{-2}	1.58×10^{-2}	4.69×10^{-2}	297.4
Ascension Island	7/12/89	3.5-45.0	2.52×10^{-2}	2.09×10^{-2}	4.29×10^{-3}	20.5
Ascension Island	7/13/89	0.5-45.0	1.62×10^{-2}	3.47×10^{-2}	-1.85×10^{-2}	-53.2
Ascension Island	7/16/89	2.5-45.0	4.70×10^{-3}	2.55×10^{-2}	-2.08×10^{-2}	-81.6
Ascension Island	7/17/89	3.5-45.0	1.10×10^{-2}	2.09×10^{-2}	-9.90×10^{-3}	-47.4
Tahiti Island	7/14/89	6.5-45.0	3.47×10^{-3}	9.46×10^{-3}	-5.99×10^{-3}	-63.3
Tahiti Island	8/27/89	4.5-45.0	4.63×10^{-3}	1.67×10^{-2}	-1.20×10^{-2}	-72.2

Table 11. Summary of SAGE-AVHRR Comparisons

LOCATION	DATE	τ_{AVHRR}	V_{inf}	V_{obs}	τ_{SAGE}	τ_{model}	H_{min}	V_{cor}
Sicily	7/3/89	0.245	17	9	0.0102	0.0425	4.5	13
Sicily	7/28/89*	0.193	24	13	0.0095	0.0328	2.5	18
Tahiti	7/14/89	0.013	>150	39	0.0091	0.0242	6.5	>150
Tahiti	8/28/89*	0.029	>150	32	0.0110	0.0425	4.5	>150
Ascension	10/3/88**	0.129	34	39	0.0207	0.0252	2.5	30
Ascension	7/13/89	0.000	>150	78	0.0080	0.0425	4.5	>150

* SAGE measurement on previous day

** SAGE measurement two days later

considerably below the nominal uncertainty of ± 0.05 in the measurements. For the other five cases, V_{cor} is still larger than the observed meteorological range, V_{obs}, suggesting that our model optical thicknesses, which may be too large, cannot account for all the differences in the results summarized in Table 6 and Figure 6. That is, some of the possible other explanations discussed in Section 5.2 must also apply. In the three cases with the largest discrepancy (with V_{inf} >150 km), the AVHRR optical depths are considerably smaller than the uncertainty of the data.

6. SUMMARY AND RECOMMENDATIONS

6.1 Summary

This report has used aerosol optical depths from NOAA/AVHRR satellites to estimate the surface meteorological range over oceans. To do this, we developed a lookup table of optical depth versus meteorological range which is based on the aerosol extinction profiles of Shettle and Fenn[4]. To better simulate conditions over oceans, we lowered the boundary layer height to 0.5 km and added an extinction profile corresponding to a 150 km meteorological range. We then applied our algorithm to aerosol optical depth data near selected island locations, and validated the inferred meteorological ranges against surface observations. For a number of reasons, however, surface visibility data at many island locations could not be used for validation. (Future studies should include more stations if possible.) Our results show reasonable success in locating regions where meteorological ranges exceed 30 km, but more precise classification may not be possible due to uncertainties in both the measurements and observations. The algorithm tends to produce higher than observed meteorological ranges, when the observed values are less than 30 km. Limited comparisons with SAGE II data suggest that the assumed model aerosol

extinction profiles used by the algorithm may contain too much aerosol loading above the boundary layer, which could account for some, but not all, of this discrepancy. Other explanations include the possibility the island sites have lower visibilities than the surrounding open ocean or the AVHRR optical depths are too small.

6.2 Recommendations for Future Research

6.2.1 Additional Supporting Measurements

The results from this effort suggest limited success in obtaining surface meteorological ranges from satellite aerosol optical depth measurements, especially in times of moderate aerosol loading. The reasons for limited success include tenuous assumptions in our algorithm and uncertainties in measurements of aerosol optical depth and surface visibility. Future research should try to determine why we are not getting better results. To achieve this, we recommend similar studies be conducted in which potential sources of error are minimized whenever possible. For example, we could apply our lookup table to optical depth measurements made with a sun photometer located near a station making surface visibility measurements. This would allow for a more meaningful comparison between inferred and observed meteorological ranges given that, in the present study, inferred meteorological ranges are based on optical depths covering $5^\circ \times 5^\circ$ regions. Also, a well-calibrated sun photometer would likely minimize errors associated with measurements of optical depth since AVHRR optical depths are only accurate to ± 0.05. This additional research could involve new measurements of aerosol optical depth and/or access existing databases of aerosol optical depth such as those from White Sand Missile Range, Ascension Island and Mauna Loa.

The recommended research would help explain the limited success in the current study. That is, continued poor agreement between inferred and observed meteorological ranges would indicate that our lookup table, and hence the aerosol extinction profiles, needs modification.

6.2.2 Oceanic Regions Influenced by Desert Dust

The aerosol profiles adopted in this report represent a clean atmosphere above the ocean boundary layer. However appreciable aerosol loading can exist over oceanic regions subject to outflow from deserts in Africa, the Middle East and eastern Asia. In the northern equatorial Atlantic, for example, highest aerosol concentrations are typically found near 5 km because the Saharan dust layer is

undercut by cooler trade wind air (Carlson and Benjamin[14]). Although particle fallout leads to reduced surface visibility below the dust cloud, it is clear that our lookup table is not applicable to these regions.

Based on the above considerations, an additional lookup table needs to be developed for regions strongly affected by desert dust. Aerosol profiles would be peaked, with their maximum concentration several kilometers above the surface. Additionally, due to particle fallout, the surface extinction would be proportional to the amount of dust loading (see Figure 7). A family of curves could be developed for various outflow regions because the height and vertical extent of dust layers are regionally dependent. Also the cloud screening algorithm will remove the regions with the strongest dust outbreaks, where the optical depth exceeds 1.0. For regions known to be influenced by desert dust, the resulting lookup tables would then replace the lookup table given Table 2 of this report.

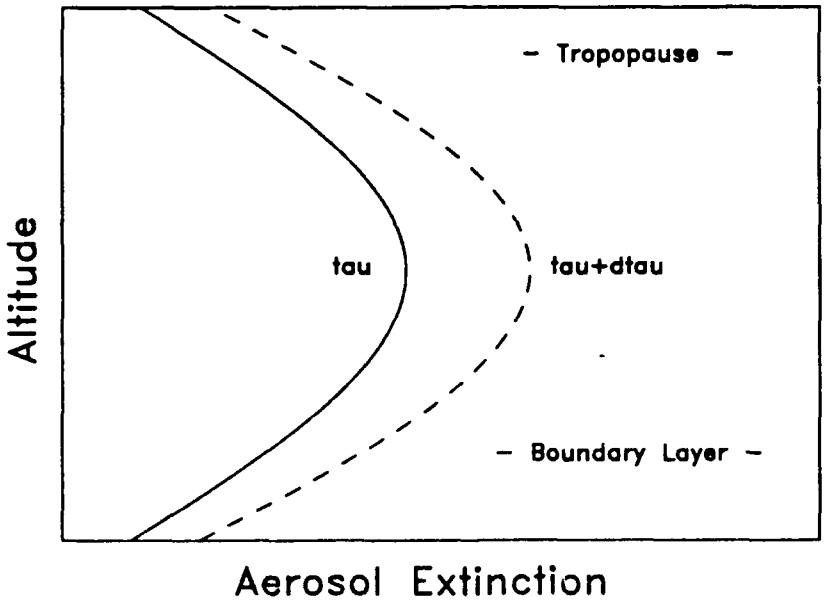

Figure 7. Aerosol Profiles for Oceanic Regions Influenced by Desert Outflow

Given the nature of the AVHRR aerosol product, it also seems reasonable to try to track dust outbreaks as they migrate from their desert source regions. Such studies have been conducted successfully by Rao *et al.*[2] By itself however, the AVHRR aerosol product must be used cautiously when attempting to identify dust

[14] Carlson, T.N. and Benjamin, S.G. (1980) Radiative Heating Rates for Saharan Dust, *J. Atmos. Sci.*, **37**: 193-213.

outbreaks over oceans. That is, the AVHRR cloud screening algorithm readily removes most clouds, but thin and subvisual cirrus having optical depths less than 0.25 could be interpreted as dust. Clearly, additional data from the suspect region, such as surface measurements or a knowledge of the synoptic scale air flow, would confirm the presence of dust.

REFERENCES

1. NOAA/NESDIS (1986) *NOAA Polar Orbiter Data (TIROS-N, NOAA-6, NOAA-7, NOAA-8, NOAA - 9, and NOAA-10) Users Guide*, Compiled and Edited by K. B. Kidwell (Revised January 1988), National Climatic Data Center Satellite Data Services Division, Washington, D.C.
2. Rao, C.R.N., Stowe, L.L., McClain, E.P., and Sapper, J. (1988) Development and Application of Aerosol Remote Sensing with AVHRR Data from the NOAA Satellites, in *Aerosols and Climate*, Hobbs, P. and McCormick, M.P. (Eds.), A. Deepak Publishing, Hampton, VA, 69-79.
3. Griggs, M. and Stowe, L.L. (1984) Measurements of Aerosol Optical Parameters from Satellites, *IRS' 84: Current Problems in Atmospheric Radiation*, G. Fiocco (Ed.), A. Deepak Publishing, Hampton, VA, 42-45.
4. Shettle, E.P. and Fenn, R.W. (1976) Models of the Atmospheric Aerosols and Their Optical Properties, in AGARD Conference Proceedings No. 183 *Optical Propagation in the Atmosphere* presented at the Electromagnetic Wave Propagation Panel Symposium, Lyngby, Denmark, 27-31 October 1975, AGARD-CP-183, (AD A028-615).
5. Oke, T.R. (1978) *Boundary Layer Climates*, Methuen Publishing, New York, 89-90.
6. Gathman, S.G, de Leeuw, G., Davidson, K.L., and Jensen, D.R. (1979) The Naval Oceanic Vertical Aerosol Model: Progress Report, in AGARD Conference Proceedings *Atmospheric Propagation in the UV, Visible, IR and MM-Wave Region and Related System Aspects*, presented at 45th Symposium Electromagnetic Wave Propagation Panel, Copenhagen Denmark, 9-13 October 1989.
7. Fenn, R.W., Clough, S.A., Gallery, W.O., Good, R.E., Kneizys, F.X., Mill, J.D., Rothman, L.S., Shettle, E.P., and Volz, F.E. (1985) Optical and Infrared Properties of the Atmosphere, Chapter 18 in *Handbook of Geophysics and the Space Environment*, A.S. Jursa Scientific Ed., Air Force Geophysics Laboratory, Hanscom AFB, MA, AFGL-TR-85-0315, (AD A167000).
8. USAFETAC (1986) DATSAV2 Surface Climatic Database Users Handbook No. 4, available from USAFETAC, Federal Building, Asheville, N.C.
9. Gordon, J.I. (1979) "Daytime Visibility, A Conceptional Review," Air Force Geophysics Laboratory, Hanscom AFB, MA, AFGL-TR-79-0257, (AD A08544-51).
10. Mauldin III, L.E., Zaun, N.H., McCormick, M.P., Guy, J.H., and Vaughn, W.R. (1985) Stratospheric Aerosol and Gas Experiment II Instrument: A Functional

Description, *Opt. Engineering*, **24**: 307-312.

11. McCormick, M.P., Hamill, P., Pepin, T.J., Chu, W.P., Swissler, T.J., and McMaster, L.R. (1979) Satellite Studies of the Stratospheric Aerosol, *Bull. Amer. Meteor. Soc.*, **60**: 1038-1046.
12. Russell, P.B. and McCormick, M.P. (1989) SAGE II Aerosol Data Validation and Initial Data Use: An Introduction and Overview, *J. Geophys. Res.*, **94**: 8335-8338.
13. Shettle, E.P. and Fenn, R.W. (1979), "Models of the Aerosols of the Lower Atmosphere and the Effects of Humidity Variations," Hanscom AFB, MA, AFGL-TR-79-0214, (AD A085615).
14. Carlson, T.N. and Benjamin, S.G. (1980) Radiative Heating Rates for Saharan Dust, *J. Atmos. Sci.*, **37**: 193-213.

Appendix A
Description of Aerosol Observation Files

This appendix describes, in detail, the structure of NOAA/NESDIS archive tapes containing aerosol optical depth data.* These archive tapes are nine track binary tapes at 6250 BPI.

The first file on each archive tape is the Header File which consists of one 400 byte physical record. (Here one byte equals 8 bits and one word equals 32 bits.) General information about the tape is contained in the Header File. The format of the Header File is given in Table A-1.

The second file on each archive tape, the Aerosol Observation File, consists of 4002 physical records, each 13024 bytes in length. The first record is the directory record which gives the record locations where optical depth data are stored for each of the 2592 blocks. To calculate the block number for a particular location, the following expression is used:

$$IBLOCK = 72 * (ILAT + 90)/5 + (ILON + 180)/5 + 1 \qquad (A-1)$$

where ILAT and ILON are respectively lower left latitude (+N,-S) and longitude (+E,-W) of the 5° block containing the desired latitude and longitude. Given the location (18.5N,66.0W), for example, ILAT = 15 and ILON = -70. Note that each block includes the minimum whole latitude and longitude and excludes the maximum whole latitude and longitude that border the block. For example, the limits of block 1 are -90.0 to -85.01 and -180.0 to -175.01. The format of the directory record is given in Table A-2.

The remaining 4001 records in the Aerosol Observation File are data records, each containing a subblock directory followed by observations of aerosol optical depth. The format of the subblock directory is given in Table A-3. To calculate the subblock number for a particular location, the following expression is used:

$$SBN = 5 * (IY - ILAT) + (IX - ILON) + 1 \qquad (A-2)$$

where IY and IX are respectively lower left latitude and longitude of the 1° block containing the desired latitude and longitude. Whenever a subblock does not contain optical depth data, the start and end position in the subblock directory contain a 0.

* McCown, S. (1989) Aerosol Observation File: TD-9614, NOAA/NESDIS Customer Services/User Services Branch, Personal Communication.

Usually only one data record is needed to store all of the optical depth data for a 5° by 5° block. In some cases, however, additional data records must be allocated as needed. Here the additional data records include subblock directories. When an entire subblock cannot fit into one record, it is split and the remainder of the subblock is put into an additional data record. Unused portions of data records and data records containing no data are 0 filled.

As indicated in Table A-3, halfwords 61 through 6512 in each data record contain individual observations of aerosol optical depth. Each observation consists of a minimum of 28 halfwords to a maximum of 48 halfwords. The first 6 halfwords contain identification information about the type of algorithm used, the satellite, time, and location. The observation format is given in Table A-4.

Table A-1. Format of the Header File

Half Word	# Bytes	Description		Range
1-40	80	Title of data set archived in File 2 of this tape		1-80 characters with blank fill
41-54	28	Data set name of disk data set		1-28 characters with blank fill
55-58	8	Original archive tape number		1-8 characters with blank fill
59-60	1	Year		0-99
	1	Month	Date of earliest	1-12
	1	Day	data on tape	1-31
	1	Blank		
61-62	1	Year		0-99
	1	Month	Date of most current	1-12
	1	Day	data on tape	1-31
	1	Blank		
63-64	4	Year		0-99
65-66	4	Month	Date and time when	1-12
67-68	4	Day	data was archived	1-31
69-70	4	Hour	from disk to tape	0-23
71-72	4	Minute		0-59
73-74	4	Second		0-59
75-76	4	Number of records of data in File 2 of tape		
77-78	4	Number of files of data on the tape (not counting Header file)		
79-200	244	Spare		

Table A-2. Format of the Directory Record

Half Word	Description	Range
1	Latitude origin	- 90
2	Longitude origin	-180
3	Size of block in latitudinal direction	In degrees currently 5
4	Size of block in longitudinal direction	In degrees currently 5
5	First free record pointer	Points to first available record
6	Number of records in file	Currently 4002
7	Halfword number of start of block directory table	Currently 11
8	Day of year of latest data	1-366
9	File availability	0 = available 1 = unavailable, update in progress
10	Year of century of latest data	0-99
11	Record number for block 1	2-4002
12	Record number for block 2	0 if no data in block
.	.	
.	.	
.	.	
2602	Record number for block 2592	

Table A-3. Format of the Subblock Directory. A subblock directory is found at the beginning of each data record

Half Word	Description	Range
1	Record number	2-4002
2	Block number	1-2592
3	Extent number (# of records removed from primary)	0 if primary
4	Pointer to succeeding overflow record	0 if no overflow. Last overflow record points to primary.
5	Pointer to halfword position of start of observation data	61 currently
6	Pointer to start of sub-block directory	11 currently
7	Lower left latitude of block	degrees
8	Lower left longitude of block	degrees
9	Pointer to last halfword containing data	If not data in the record, this pointer points to the start position of observation data -1.
10	Unused	
11	Halfword of start of data for sub-block #1	0 if no data for this sub-block in this record.
12	Halfword of end of data for sub-block # 1	0 if no data for this sub-block in this record. Other extents may or may not contain data for this sub-block.
13 - 60	Similar to halfwords 11 and 12 for remaining sub-blocks	
61 - 6512	Observation data	

Table A-4. Format of the Observation Data. This format is repreated for each observation in the data record

Half Word	# Bytes	Description	Range
1	1	Type of observation	129 - 255
1	1	Source of observation	0 - 255
2	1	Year of century	0 - 99
2	1	Month of year	1 - 12
3	2	Latitude (+N, -S)*100	-9,000 to 9,000
4	2	Longitude (+E, -W) *100	-18,000 to 17,999
5	1	Day of month	1 - 31
5	1	Hour of day	0 - 23
6	1	Minute of hour	0 - 59
6	1	Second of minute	0 - 59
7	2	Aerosol corrected SST	-20 to 350 (°C *10)
8	2	Reliability	0 to 32,767
9	2	Solar zenith angle (°C *10) (Negative to left of spacecraft track, positive to right)	0 to 1800
10	2		
11	2	Analyzed field SST (°C *10)	-20 to 350
12	2	Internal error (RMS*100)	0 to 1000
13	2	Relative azimuth angle (°C*10)	0 to 1800
14	2	Climatological SST (°C*10)	-20 to 350
15	1	Beginning row of unit array	1 - 11
15	1	Beginning column of unit array	1 - 11
16	2	AVHRR Channel 1 average (%*100)	0 - 10,000
17	2	AVHRR Channel 2 average (%*100)	0 - 10,000
18	2	AVHRR Channel 3 average (°K *100)	0 - 32,767
19	2	AVHRR Channel 4 average (°K *100)	0 - 32,767
20	2	AVHRR Channel 5 average (°K *100)	0 - 32,767
21	2	Space view SDEV Channel 1 (% *100)	0 - 10,000
22	2	Space view SDEV Channel 2 (% *100)	0 - 10,000

Table A-4. (cont'd.)

Half Word	# Bytes	Description	Range
23	2	Space view SDEV Channel 3 (°K *100)	0 - 32,767
24	2	Space view SDEV Channel 4 (°K *100)	0 - 32,767
25	2	Space view SDEV Channel 5 (°K *100)	0 - 32,767
26	2	Algorithm number	1011 to ?
27	2	Aerosol optical thickness *1000	0 - 2440
28	2	Uncorrected SST (°K *100)	27,116 - 30,816
		IF HIRS DATA ARE APPENDED	
29	2	HIRS Channel 1 temp (°K *100)	0 - 32,767
30	2	HIRS Channel 2 temp (°K *100)	0 - 32,767
31	2	HIRS Channel 3 temp (°K *100)	0 - 32,767
32	2	HIRS Channel 4 temp (°K *100)	0 - 32,767
33	2	HIRS Channel 5 temp (°K *100)	0 - 32,767
34	2	HIRS Channel 6 temp (°K *100)	0 - 32,767
35	2	HIRS Channel 7 temp (°K *100)	0 - 32,767
36	2	HIRS Channel 8 temp (°K *100)	0 - 32,767
37	2	HIRS Channel 9 temp (°K *100)	0 - 32,767
38	2	HIRS Channel 10 temp (°K *100)	0 - 32,767
39	2	HIRS Channel 11 temp (°K *100)	0 - 32.767
40	2	HIRS Channel 12 temp (°K *100)	0 - 32,767
41	2	HIRS Channel 13 temp (°K *100)	0 - 32,767
42	2	HIRS Channel 14 temp (°K *100)	0 - 32,767
43	2	HIRS Channel 15 temp (°K *100)	0 - 32,767
44	2	HIRS Channel 16 temp (°K *100)	0 - 32,767
45	2	HIRS Channel 17 temp (°K *100)	0 - 32,767
46	2	HIRS Channel 18 temp (°K *100)	0 - 32,767
47	2	HIRS Channel 19 temp (°K *100)	0 - 32,767
48	2	HIRS Channel 20 temp (°K *100)	0 - 32,767

Appendix B
Description of Programs and Tapes

A number of Fortran computer programs have been developed to read and process the AVHRR aerosol optical depth data. This appendix briefly describes these programs, as well as computer tapes developed during this effort. Except for the programs that read magnetic tapes, standard Fortran 77 coding procedures are used. Generally, the programs were developed on the AFGL CYBER computer system and, therefore, users should have a working knowledge of CYBER computer systems. Table B-1 lists the programs developed during this effort, plus their input and output files. Table B-1 also contains three programs to read and process aerosol data from the Stratospheric and Gas Experiment II (SAGE II). A flow diagram for reading and processing the aerosol optical depth data is shown in Figure B-1.

Five of the programs listed in Table B-1 read data from magnetic tapes. They are FRDAVHR, FRDDATS, FRDSAG1, FRDSAG2 and FRDSAG3. Before these programs can be executed, the desired tape must be physically mounted on a tape drive by AFGL computer personnel. This is acheived on the CYBER by entering

```
LABEL,TAPE1,VSN=CCxxxx,PO=R,LB=KL,D=GE,F=L
```

or

```
LABEL,TAPE1,VSN=Mxxxx,PO=R,LB=KU,D=GE,F=L
```

where xxxx is the tape number. This command assigns the logical name TAPE1 to the magnetic tape. Also, a CYBER Fortran library must be defined before the programs FRDAVHR and FRDDATS can be executed. This is done by entering

```
GET,TAPESYS/UN=PLIB
LIBRARY,TAPESYS.
```

Upon program completion, the magnetic tape must be dismounted from the tape drive using

```
RETURN,TAPE1.
```

The program FRDAVHR should be run in batch mode. At most, it takes about 300 CPU seconds to read through one AVHRR tape and the output file is typically about 7500 PRUs (6 megabytes) in size. The other programs execute quickly and can be run interactively.

Tables B-2 through B-4 list the computer tapes created during this effort. These

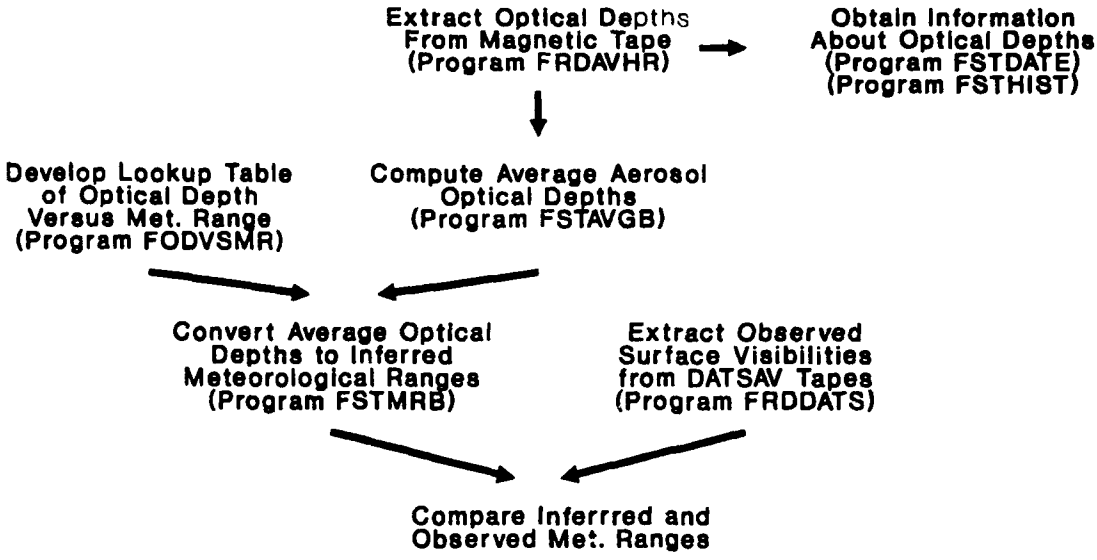

Figure B-1. Flow Diagram for Reading and Processing Aerosol Optical Depth Data

tapes contain copies of the eight day AVHRR Aerosol Observation Files, "extracted" aerosol data near nineteen island locations and DATSAV2 files. The extracted aerosol files, which are stored in AFGL computer center RECLAIM format, contain all optical depth data that fall within an AVHRR block defining an island location, or one of its eight adjacent blocks ($15^\circ \times 15^\circ$ in all).

Table B-1. Brief Description of Programs Developed in This Effort

PROGRAM NAME	INPUT	OUTPUT	BRIEF DESCRIPTION
FBLOCK	RLAT* RLON*	IBLOCK* ISUB*	Computes the AVHRR block and subblock number corresponding to the user-specified latitude and longitude
FODVSMR	IFWSS* ISTRAT* IUPAT*	DODVSMR	Develops a lookup table of aerosol optical depth versus meteorological range using standard aerosol extinction profiles
FRDAVHR	TAPE1	DAVHRR	Reads a tape containing an Eight Day Aerosol Observation File
FRDDATS	TAPE1	DATSAV2	Reads a tape containing a USAFETAC DATSAV2 File
FRDSAG1	TAPE1 ZLAT* ZLON* Fileout*	Fileout**	Reads a tape containing SAGE II aerosol data and extracts data near the user-specified latitude and longitude
FRDSAG2	TAPE1 JMM,JDD* JHH,JMN*	TAPE6	Reads a tape containing SAGE II aerosol data and extracts data for the user-specified date and time
FRDSAG3	TAPE1	TAPE6	Reads a tape containing SAGE II aerosol data and provides a listing of all available data on the tape
FSTAVGB	DAVHRR	DSTAVGB	Computes average aerosol optical depths and standard deviations near each island location
FSTBLK	None	DSTBLK	Lists the AVHRR block and adjacent blocks associated with all island locations
FSTDATE	DAVHRR	DSTDATE	Determines the days when aerosol optical depth measurements exist near the island locations
FSTHIST	DAVHRR	DSTHIST	Determines how many AVHRR measurements there are near each island location
FSTMRB	DSTAVGB	DSTMRB	Computes inferred meteorological ranges near each island location using the averaged AVHRR aerosol optical depths
JTAPECOP	None	None	Batch job for copying foreign magnetic tapes to CYBER computer center tapes
JRDAVHR	None	None	Batch job for reading an Eight Day Observation File on the CYBER
JPROCES	None	None	Batch job for processing AVHRR data after it has been read from magnetic tape

* Terminal I/O parameters

** File name determined by the user

Table B-2. Tapes Containing Eight Day Aerosol Observation Files. Each tape contains data for eight days up to and including the date shown in the table.

DATE	TAPE NO.	TAPE LABEL
October 5, 1988	CC1140	Yes
October 12, 1988	CC1377	Yes (see note 1)
October 19, 1988	CC1817	Yes
October 26, 1988	CC1821	Yes
November 2, 1988	CC1628	Yes
November 11, 1988	M10158	No
June 27, 1989	CC0673	Yes
July 5, 1989	CC0417	Yes
July 12, 1989	CC0492	Yes
July 19, 1989	CC0495	Yes
July 26, 1989	CC0435	Yes (see note 2)
August 2, 1989	CC0353	Yes
August 9, 1989	CC0264	Yes
August 16, 1989	CC0254	Yes
August 23, 1989	CC0088	Yes
August 30, 1989	CC0699	Yes
September 6, 1989	CC0709	Yes
September 13, 1989	CC1091	Yes
September 20, 1989	CC1161	Yes
September 27, 1989	CC1086	Yes
October 4, 1989	CC1010	Yes
October 11, 1989	CC2720	Yes
October 18, 1989	CC2752	Yes
October 25, 1989	CC2750	Yes
November 1, 1989	CC2735	Yes
November 8, 1989	CC2726	Yes
November 15, 1989	M10193	No
November 22, 1989	M10195	No
November 29, 1989	M10194	No
December 6, 1989	M10196	No
December 13, 1989	M10197	No
December 20, 1989	M10275	No
December 27, 1989	M10276	No
January 3, 1990	M10277	No
January 10, 1990	M10393	No
January 17, 1990	M10392	No
January 24, 1990	M10162	No
January 31, 1990	M10312	No
February 7, 1990	M10314	No
February 14, 1990	M10313	No
February 21, 1990	M10315	No
February 28, 1990	M10311	No

Note 1: missing header record
Note 2: file contains bad data records part way through

Table B-3. Tapes Containing Aerosol Data for the Island Locations. The tapes are formatted as CYBER RECLAIM tapes. Data include extracted aerosol data, a histogram of observations by block number and statistics about the aerosol optical depths near each island location.

DATE	TAPE NO.	TAPE LABEL
October 5, 1988	CC0720	Yes
October 12, 1988	CC0720	Yes
October 19, 1988	CC0720	Yes
October 26, 1988	CC0720	Yes
November 2, 1988	CC0720	Yes
November 11, 1988	M10159	Yes
June 27, 1989	CC0762	Yes
July 5, 1989	CC0766	Yes
July 12, 1989	CC0766	Yes
July 19, 1989	CC0762	Yes
July 26, 1989	CC0766	Yes
August 2, 1989	CC0766	Yes
August 9, 1989	CC0720	Yes
August 16, 1989	CC0720	Yes
August 23, 1989	CC0762	Yes
August 30, 1989	CC0762	Yes (see note 1)
September 6, 1989	CC0762	Yes (see note 1)
September 13, 1989	CC1297	Yes
September 20, 1989	CC1297	Yes
September 27, 1989	CC1297	Yes (see note 1)
October 4, 1989	CC1297	Yes
October 11, 1989	M10159	Yes
October 18, 1989	M10159	Yes
October 25, 1989	M10159	Yes
November 1, 1989	M10159	Yes
November 8, 1989	M10159	Yes
November 15, 1989	CC1622	Yes (see note 1)
November 22, 1989	CC1622	Yes
November 29, 1989	CC1622	Yes
December 6, 1989	CC1622	Yes
December 13, 1989	M10278	Yes
December 20, 1989	M10278	Yes
December 27, 1989	M10278	Yes
January 3, 1990	M10278	Yes
January 10, 1990	M10163	Yes (see note 1)
January 17, 1990	M10163	Yes
January 24, 1990	M10163	Yes
January 31, 1990	M10163	Yes (see note 1)
February 7, 1990	M10164	Yes
February 14, 1990	M10164	Yes
February 21, 1990	M10164	Yes
February 28, 1990	M10164	Yes

Note 1: extracted aerosol data files have been truncated because they are too long (>10000 PRUs)

Table B-4. Tapes Containing DATSAV2 Files

DATE	TAPE NO.	TAPE LABEL	COMMENT
September - November 1988	CC0128	Yes	Ascension Island
September - November 1988	CC0228	Yes	Other island locations
June - September 1989	CC0810	Yes	Ascension Island
June - September 1989	CC0812	Yes	Other island locations
October 1989 - February 1990	M11290	no	Ascension Island
October 1989 - February 1990	CC0633	yes	Other Island Locations

Appendix C
Daily Comparisons of Inferred and Observed Meteorological Ranges

Tables C-1 through C-7 list daily comparisons of inferred and observed meteorological ranges for the seven island locations investigated in this report. The daily comparisons were used to construct the histograms in the main text (Figures 6(a) and 6(b)). In each table, the following quantities are given:

1. Date and time of the AVHRR measurement
2. N_{obs}, number of observations used to calculate the average aerosol optical depth
3. $\overline{\tau}$, average aerosol optical depth
4. σ, accompanying standard deviation
5. ϵ, relative variation (expressed as a fraction)
6. V_{inf}, inferr ed meteorological range
7. V_{obs}, meteorological range based on the observed surface visibility

In Tables C-1 through C-7, values of V_{inf} exceeding 50 km have been set to 50 km since that is the upper limit of observed values at all sites except Ascension Island. Also 50 km is the largest meteorological range that can be meaningfully derived from the AVHRR data, since an uncertainty of ± 0.05 in optical depth corresponds to possible values of V_{inf} between 27 and 150 km.

Table C-1. Daily Comparisons of Inferred and Observed Meteorological Ranges for the Marshall Islands

DATE	TIME (GMT)	N_{obs}	$\overline{\tau}$	σ	ϵ	V_{inf}	V_{obs}
10/ 5/88	5:17:23	16	0.028	0.016	0.571	50.0	31.2
10/ 6/88	5: 6:16	92	0.004	0.013	3.250	50.0	31.2
10/ 7/88	4:55:30	43	0.008	0.015	1.875	50.0	31.2
10/ 8/88	4:45: 9	4	0.018	0.020	1.111	50.0	31.2
10/16/88	4:57:25	59	0.005	0.012	2.400	50.0	25.7
10/17/88	4:46:32	35	0.001	0.004	4.000	50.0	31.2
10/24/88	5:10:26	62	0.005	0.014	2.800	50.0	25.0
6/21/89	2:29:27	2	0.068	0.017	0.250	50.0	31.2
6/26/89	3:19:24	12	0.025	0.020	0.800	50.0	31.2
6/27/89	3: 8:25	61	0.001	0.007	7.000	50.0	31.2
6/28/89	2:58: 3	77	0.007	0.016	2.286	50.0	31.2
7/ 7/89	3: 5:44	49	0.019	0.024	1.263	50.0	18.7
7/10/89	2:35:26	1	0.194	0.000	0.000	23.4	31.2
7/16/89	3:13:13	37	0.002	0.008	4.000	50.0	31.2
7/25/89	3:20:48	12	0.037	0.008	0.216	50.0	31.2
8/ 8/89	2:36:24	23	0.013	0.022	1.692	50.0	31.2
8/13/89	3:26:14	1	0.027	0.000	0.000	50.0	31.2
8/24/89	3:11:37	26	0.015	0.020	1.333	50.0	31.2
8/25/89	3: 0:50	62	0.015	0.020	1.333	50.0	31.2
8/26/89	2:51:33	2	0.068	0.024	0.353	50.0	31.2
9/ 2/89	3:18:20	3	0.029	0.004	0.138	50.0	31.2
9/ 3/89	3: 7:52	68	0.002	0.008	4.000	50.0	31.2
9/ 4/89	2:57:18	38	0.014	0.021	1.500	50.0	31.2
9/12/89	3:14:49	27	0.013	0.019	1.462	50.0	31.2
9/13/89	3: 4:15	86	0.003	0.009	3.000	50.0	31.2
9/14/89	2:53:53	91	0.007	0.013	1.857	50.0	31.2
9/22/89	3:10:57	24	0.005	0.014	2.800	50.0	31.2
9/23/89	3: 0:30	78	0.004	0.008	2.000	50.0	15.6
9/25/89	2:39:35	35	0.009	0.019	2.111	50.0	31.2
10/ 4/89	2:47:22	1	0.219	0.000	0.000	16.7	31.2
10/ 5/89	2:35:51	14	0.022	0.023	1.045	50.0	31.2
10/10/89	3:24: 5	18	0.009	0.014	1.556	50.0	31.2
10/11/89	3:13:36	18	0.009	0.019	2.111	50.0	31.2
10/12/89	3: 3: 2	76	0.003	0.011	3.667	50.0	31.2
10/15/89	2:31:58	1	0.307	0.000	0.000	11.6	14.6
10/20/89	3:20: 0	5	0.004	0.005	1.250	50.0	31.2
10/21/89	3:10:11	2	0.006	0.008	1.333	50.0	31.2
10/29/89	3:27: 9	2	0.000	0.000	-	50.0	31.2
10/30/89	3:15:25	24	0.014	0.018	1.286	50.0	31.2
11/ 1/89	2:54:16	105	0.014	0.024	1.714	50.0	31.2

Table C-1. (cont)

DATE	TIME (GMT)	N_{obs}	$\overline{\tau}$	σ	ϵ	V_{inf}	V_{obs}
11/ 3/89	2:33:21	29	0.009	0.018	2.000	50.0	31.2
11/18/89	3:17:39	3	0.000	0.000	-	50.0	24.9
11/19/89	3: 6:52	7	0.008	0.010	1.250	50.0	31.2
11/20/89	2:56:25	1	0.006	0.000	0.000	50.0	31.2
12/ 6/89	3:27: 9	25	0.008	0.015	1.875	50.0	31.2
12/ 8/89	3: 5:36	15	0.037	0.021	0.568	50.0	31.2
12/10/89	2:45:38	1	0.116	0.000	0.000	41.1	31.2
12/17/89	3:10:56	50	0.014	0.018	1.286	50.0	31.2
12/27/89	3: 5: 4	39	0.008	0.016	2.000	50.0	31.2
1/ 5/90	3:10:54	7	0.069	0.018	0.261	50.0	31.2
1/ 7/90	2:48:55	5	0.216	0.064	0.296	17.0	31.2
1/13/90	3:25:44	3	0.050	0.012	0.240	50.0	31.2
1/16/90	2:53: 3	5	0.216	0.029	0.134	17.0	31.2
1/24/90	3: 7:54	10	0.168	0.046	0.274	22.5	31.2
1/25/90	2:57:39	2	0.317	0.013	0.041	11.2	31.2
1/26/90	2:47: 5	3	0.277	0.090	0.325	13.0	31.2
2/ 1/90	3:23: 4	2	0.073	0.014	0.192	50.0	31.2
2/10/90	3:26:55	1	0.061	0.000	0.000	50.0	15.6
2/19/90	3:31:30	8	0.034	0.022	0.647	50.0	31.2
2/20/90	3:21:34	3	0.072	0.016	0.222	50.0	31.2
2/21/90	3: 9:49	40	0.023	0.024	1.043	50.0	31.2
2/24/90	2:37:55	4	0.010	0.010	1.000	50.0	31.2

Table C-2. Daily Comparisons of Inferred and Observed Meteorological Ranges for Honolulu, HI

DATE	TIME (GMT)	N_{obs}	$\overline{\tau}$	σ	ϵ	V_{inf}	V_{obs}
10/ 2/88	2:31: 4	721	0.002	0.008	4.000	50.0	52.0
10/ 3/88	2:20: 5	512	0.001	0.006	6.000	50.0	52.0
10/10/88	2:44:19	86	0.003	0.009	3.000	50.0	40.3
10/11/88	2:33: 6	651	0.004	0.014	3.500	50.0	40.3
10/12/88	2:22: 6	474	0.003	0.013	4.333	50.0	45.5
10/13/88	2:11:52	13	0.001	0.003	3.000	50.0	31.2
10/20/88	2:35: 1	181	0.003	0.009	3.000	50.0	45.5
10/21/88	2:24: 1	93	0.011	0.022	2.000	50.0	40.3
10/22/88	2:13:41	50	0.013	0.019	1.462	50.0	40.3
6/21/89	0:51:27	59	0.008	0.015	1.875	50.0	40.3
6/22/89	0:40:53	91	0.034	0.024	0.706	50.0	40.3
6/30/89	0:59:21	10	0.043	0.009	0.209	50.0	40.3
7/ 1/89	0:48:35	162	0.024	0.019	0.792	50.0	40.3
7/ 2/89	0:38:13	171	0.017	0.022	1.294	50.0	52.0
7/10/89	0:56: 9	59	0.032	0.020	0.625	50.0	40.3
7/11/89	0:45:48	82	0.040	0.024	0.600	50.0	40.3
7/12/89	0:35:27	176	0.090	0.022	0.244	50.0	40.3
7/14/89	0:14:25	161	0.143	0.037	0.259	44.0	40.3
7/15/89	0: 4:23	17	0.168	0.028	0.167	30.7	40.3
7/29/89	1: 1: 4	1	0.095	0.000	0.000	50.0	40.3
7/30/89	0:50:30	82	0.043	0.020	0.465	50.0	40.3
7/31/89	0:39:56	156	0.051	0.024	0.471	50.0	40.3
8/ 2/89	0:19: 0	261	0.106	0.034	0.321	50.0	31.2
8/ 8/89	0:58: 4	10	0.028	0.010	0.357	50.0	40.3
8/ 9/89	0:47:18	68	0.042	0.018	0.429	50.0	40.3
8/11/89	0:26:22	514	0.027	0.023	0.852	50.0	52.0
8/18/89	0:54:33	54	0.015	0.015	1.000	50.0	40.3
8/19/89	0:44: 5	150	0.016	0.016	1.000	50.0	40.3
8/22/89	0:13:59	7	0.173	0.036	0.208	29.0	46.8
8/23/89	0: 3: 6	26	0.059	0.024	0.407	50.0	52.0
8/27/89	1: 1:36	9	0.000	0.000	-	50.0	52.0
8/28/89	0:51: 8	140	0.000	0.002	-	50.0	46.8
8/29/89	0:40:40	249	0.002	0.007	3.500	50.0	45.5
8/30/89	0:30:13	107	0.014	0.021	1.500	50.0	52.0
9/ 6/89	0:58:30	10	0.004	0.010	2.500	50.0	40.3
9/ 7/89	0:47:43	96	0.005	0.008	1.600	50.0	40.3
9/ 8/89	0:37:22	224	0.007	0.015	2.143	50.0	40.3
9/ 9/89	0:26:41	399	0.022	0.019	0.864	50.0	46.8
9/16/89	0:54:33	54	0.005	0.013	2.600	50.0	40.3
9/18/89	0:33:31	474	0.004	0.010	2.500	50.0	52.0

Table C-2. (cont.)

DATE	TIME (GMT)	N_{obs}	$\overline{\tau}$	σ	ϵ	V_{inf}	V_{obs}
9/19/89	0:22:57	567	0.016	0.022	1.375	50.0	52.0
9/25/89	1: 1:22	12	0.000	0.000	-	50.0	31.2
9/26/89	0:50:42	113	0.006	0.014	2.333	50.0	40.3
9/27/89	0:40:14	255	0.005	0.012	2.400	50.0	40.3
9/28/89	0:29:40	471	0.002	0.006	3.000	50.0	52.0
10/ 5/89	0:57:13	30	0.005	0.016	3.200	50.0	26.0
10/ 6/89	0:46:45	162	0.002	0.009	4.500	50.0	35.1
10/ 7/89	0:36:11	366	0.000	0.004	-	50.0	35.1
10/ 8/89	0:25:43	672	0.001	0.006	6.000	50.0	35.1
10/ 9/89	0:15: 8	951	0.002	0.009	4.500	50.0	35.1
10/14/89	1: 4: 1	1	0.000	0.000	-	50.0	40.3
10/16/89	0:42:53	73	0.004	0.012	3.000	50.0	31.2
10/17/89	0:32:12	405	0.002	0.010	5.000	50.0	31.2
10/18/89	0:21:31	319	0.007	0.018	2.571	50.0	46.8
10/24/89	0:59:19	44	0.027	0.017	0.630	50.0	46.8
10/25/89	0:49:30	12	0.029	0.016	0.552	50.0	46.8
10/26/89	0:38:11	215	0.003	0.009	3.000	50.0	40.3
10/27/89	0:27:37	655	0.002	0.010	5.000	50.0	41.6
10/28/89	0:17: 8	874	0.006	0.019	3.167	50.0	35.1
10/29/89	0: 6:22	595	0.004	0.015	3.750	50.0	35.1
11/ 3/89	0:54:50	173	0.000	0.003	-	50.0	41.6
11/ 4/89	0:44:10	106	0.006	0.021	3.500	50.0	40.3
11/ 8/89	0: 1:40	105	0.017	0.019	1.118	50.0	35.1
11/14/89	0:39:41	3	0.048	0.017	0.354	50.0	31.2
11/16/89	0:18: 1	17	0.019	0.016	0.842	50.0	31.2
11/17/89	0: 8:30	70	0.000	0.003	-	50.0	10.4
11/22/89	0:55:54	23	0.010	0.014	1.400	50.0	40.3
11/23/89	0:45: 1	465	0.003	0.007	2.333	50.0	35.1
11/24/89	0:34:14	611	0.000	0.003	-	50.0	40.3
11/25/89	0:23:39	738	0.000	0.004	-	50.0	35.1
11/26/89	0:13:12	704	0.000	0.004	-	50.0	35.1
11/27/89	0: 2:12	491	0.000	0.000	-	50.0	35.1
12/ 6/89	0: 7:26	1006	0.003	0.013	4.333	50.0	36.4
12/10/89	1: 6:15	11	0.026	0.018	0.692	50.0	35.1
12/11/89	0:55:22	58	0.008	0.011	1.375	50.0	15.6
12/12/89	0:44:42	54	0.010	0.011	1.100	50.0	35.1
12/13/89	0:34: 1	359	0.001	0.006	6.000	50.0	35.1
12/14/89	0:23:20	383	0.007	0.015	2.143	50.0	35.1
12/15/89	0:12:33	279	0.011	0.017	1.545	50.0	35.1
12/16/89	0: 1:53	75	0.002	0.005	2.500	50.0	35.1

Table C-2. (cont.)

DATE	TIME (GMT)	N_{obs}	$\overline{\tau}$	σ	ϵ	V_{inf}	V_{obs}
12/21/89	0:50:15	131	0.006	0.013	2.167	50.0	26.0
12/22/89	0:38:56	494	0.000	0.002	-	50.0	35.1
12/23/89	0:28:15	1225	0.001	0.006	6.000	50.0	29.9
12/24/89	0:17:40	1908	0.002	0.013	6.500	50.0	41.6
12/25/89	0: 6:54	555	0.001	0.007	7.000	50.0	35.1
12/29/89	1: 5:11	9	0.000	0.000	-	50.0	35.1
12/30/89	0:54:37	119	0.007	0.013	1.857	50.0	31.2
12/31/89	0:43:44	307	0.001	0.006	6.000	50.0	35.1
1/ 1/90	0:33: 3	472	0.003	0.010	3.333	50.0	35.1
1/ 2/90	0:22:20	841	0.009	0.018	2.000	50.0	41.6
1/ 3/90	0:11:34	659	0.009	0.018	2.000	50.0	36.4
1/ 4/90	0: 1:32	32	0.004	0.010	2.500	50.0	36.4
1/ 8/90	0:59:11	133	0.001	0.004	4.000	50.0	41.6
1/ 9/90	0:48:24	182	0.005	0.012	2.400	50.0	41.6
1/10/90	0:37:37	220	0.008	0.016	2.000	50.0	31.2
1/11/90	0:26:56	195	0.011	0.017	1.545	50.0	41.6
1/12/90	0:16:22	545	0.008	0.019	2.375	50.0	41.6
1/18/90	0:52:47	2	0.074	0.009	0.122	50.0	6.5
1/28/90	0:47:39	4	0.060	0.016	0.267	50.0	20.8
2/ 1/90	0: 3:53	48	0.088	0.022	0.250	50.0	41.6
2/ 5/90	1: 1:25	54	0.020	0.024	1.200	50.0	31.2
2/ 6/90	0:50:38	177	0.015	0.018	1.200	50.0	46.8
2/14/90	1: 5:35	59	0.000	0.001	-	50.0	41.6
2/16/90	0:44: 1	457	0.009	0.014	1.556	50.0	31.2
2/17/90	0:33:20	693	0.003	0.010	3.333	50.0	31.2
2/25/90	0:49: 8	52	0.001	0.003	3.000	50.0	31.2

Table C-3. Daily Comparisons of Inferred and Observed Meteorological Ranges for Cantania, Sicily

DATE	TIME (GMT)	N_{obs}	$\overline{\tau}$	σ	ϵ	V_{inf}	V_{obs}
10/ 3/88	14:19: 7	8	0.293	0.026	0.089	12.2	13.0
6/22/89	12:40: 8	356	0.139	0.029	0.209	47.2	13.0
6/23/89	12:29:34	672	0.150	0.040	0.267	39.2	10.4
6/24/89	12:19: 7	506	0.178	0.037	0.208	27.4	19.5
6/25/89	12: 9:50	5	0.208	0.032	0.154	21.2	18.2
6/29/89	13: 8:38	82	0.206	0.032	0.155	21.5	13.0
7/ 2/89	12:37:21	337	0.154	0.034	0.221	37.0	13.0
7/ 3/89	12:26:48	75	0.245	0.066	0.269	17.2	9.1
7/ 4/89	12:16:20	346	0.122	0.033	0.270	50.0	19.5
7/ 9/89	13: 5:51	39	0.216	0.029	0.134	20.2	13.0
7/11/89	12:45: 3	86	0.214	0.060	0.280	20.4	13.0
7/12/89	12:34:28	121	0.281	0.033	0.117	14.4	9.1
7/14/89	12:13:40	116	0.182	0.043	0.236	26.3	15.6
7/28/89	13:10:20	65	0.193	0.041	0.212	23.6	13.0
7/29/89	12:59:59	57	0.277	0.061	0.220	14.7	13.0
7/30/89	12:49:25	252	0.192	0.047	0.245	23.8	6.5
7/31/89	12:39: 4	400	0.182	0.032	0.176	26.3	10.4
8/ 8/89	12:56:47	338	0.142	0.031	0.218	44.7	13.0
8/16/89	13:14:36	39	0.174	0.027	0.155	28.6	13.0
8/17/89	13: 4: 3	201	0.188	0.027	0.144	24.7	10.4
8/18/89	12:53:35	89	0.262	0.075	0.286	15.8	9.1
8/19/89	12:43: 7	103	0.299	0.069	0.231	13.4	7.8
8/20/89	12:32:39	481	0.244	0.081	0.332	17.2	10.4
8/21/89	12:22: 6	676	0.241	0.064	0.266	17.5	6.5
8/22/89	12:11:38	269	0.269	0.064	0.238	15.2	6.5
8/26/89	13:11:12	30	0.177	0.054	0.305	27.7	10.4
8/27/89	13: 0:44	118	0.167	0.041	0.246	31.1	9.1
8/28/89	12:50:10	398	0.134	0.028	0.209	50.0	19.5
9/ 7/89	12:46:45	17	0.347	0.110	0.317	11.2	10.4
9/ 8/89	12:36:17	57	0.330	0.068	0.206	11.9	6.5
9/ 9/89	12:25:49	124	0.441	0.117	0.265	8.4	7.8
9/15/89	13: 4: 9	64	0.114	0.026	0.228	50.0	10.4
9/21/89	12: 2:14	1	0.344	0.000	0.000	11.3	7.8
9/24/89	13:10:52	53	0.099	0.021	0.212	50.0	10.4
9/29/89	12:18:14	256	0.144	0.048	0.333	28.3	26.0
10/ 5/89	12:56:21	279	0.016	0.020	1.250	50.0	26.0
10/ 9/89	12:14:11	37	0.202	0.034	0.168	18.3	39.0
10/10/89	12: 4:28	17	0.116	0.030	0.259	41.1	26.0
10/13/89	13:14:41	2	0.081	0.008	0.099	50.0	5.2
10/14/89	13: 2:44	1	0.129	0.000	0.000	34.0	10.4

Table C-3. (cont.)

DATE	TIME (GMT)	N_{obs}	$\bar{\tau}$	σ	ϵ	V_{inf}	V_{obs}
10/15/89	12:52: 9	278	0.025	0.024	0.960	50.0	32.5
10/17/89	12:31: 1	673	0.008	0.018	2.250	50.0	19.5
10/18/89	12:20:33	743	0.004	0.016	4.000	50.0	19.5
10/25/89	12:47:47	288	0.084	0.025	0.298	50.0	9.1
10/29/89	12: 6: 3	69	0.115	0.020	0.174	41.8	7.8
11/10/89	13:21: 5	8	0.019	0.020	1.053	50.0	13.0
11/15/89	12:27:48	973	0.007	0.020	2.857	50.0	19.5
11/16/89	12:17: 8	121	0.007	0.020	2.857	50.0	10.4
11/21/89	13: 5:17	366	0.024	0.022	0.917	50.0	19.5
11/22/89	12:54:37	141	0.008	0.017	2.125	50.0	19.5
11/23/89	12:43:56	1	0.059	0.000	0.000	50.0	13.0
11/25/89	12:22:41	493	0.002	0.010	5.000	50.0	32.5
12/ 5/89	12:17:15	86	0.016	0.022	1.375	50.0	6.5
12/ 6/89	12: 7:20	36	0.001	0.001	1.000	50.0	3.9
12/11/89	12:54:30	254	0.006	0.014	2.333	50.0	10.4
12/12/89	12:43:43	203	0.010	0.017	1.700	50.0	13.0
12/13/89	12:33: 2	759	0.001	0.007	7.000	50.0	13.0
12/14/89	12:22:28	619	0.000	0.001	-	50.0	19.5
12/15/89	12:11:29	336	0.003	0.013	4.333	50.0	32.5
12/18/89	13:20:52	25	0.000	0.000	-	50.0	39.0
12/19/89	13:10: 5	226	0.001	0.005	5.000	50.0	39.0
12/21/89	12:48:38	292	0.001	0.005	5.000	50.0	39.0
12/22/89	12:37:57	217	0.001	0.005	5.000	50.0	10.4
12/23/89	12:27:16	508	0.000	0.002	-	50.0	19.5
12/28/89	13:16:23	1	0.068	0.000	0.000	50.0	13.0
12/29/89	13: 4:20	112	0.018	0.024	1.333	50.0	19.5
1/ 1/90	12:31:56	121	0.009	0.021	2.333	50.0	26.0
1/ 2/90	12:21:10	121	0.012	0.021	1.750	50.0	5.2
1/ 7/90	13: 8:53	46	0.033	0.019	0.576	50.0	13.0
1/ 8/90	12:58: 6	185	0.021	0.022	1.048	50.0	6.5
1/ 9/90	12:47:19	144	0.016	0.023	1.438	50.0	10.4
1/10/90	12:36:39	57	0.010	0.023	2.300	50.0	6.5
1/20/90	12:30:20	686	0.004	0.012	3.000	50.0	10.4
1/21/90	12:19:47	483	0.002	0.010	5.000	50.0	15.6
1/25/90	13:17:51	61	0.017	0.016	0.941	50.0	10.4
1/27/90	12:56:11	475	0.012	0.020	1.667	50.0	13.0
1/30/90	12:23:50	415	0.004	0.012	3.000	50.0	13.0
1/31/90	12:13: 3	244	0.010	0.014	1.400	50.0	9.1
2/ 3/90	13:22: 7	38	0.016	0.018	1.125	50.0	19.5
2/ 5/90	13: 0:21	312	0.011	0.020	1.818	50.0	9.1

Table C-3. (cont.)

DATE	TIME (GMT)	N_{obs}	$\overline{\tau}$	σ	ϵ	V_{inf}	V_{obs}
2/14/90	13: 4:37	6	0.146	0.024	0.164	27.7	19.5
2/18/90	12:21:29	777	0.004	0.017	4.250	50.0	7.8
2/22/90	13:19:33	28	0.099	0.028	0.283	50.0	7.8

Table C-4. Daily Comparisons of Inferred and Observed Meteorological Ranges for Norman Manley, Jamaica

DATE	TIME (GMT)	N_{obs}	$\overline{\tau}$	σ	ϵ	V_{inf}	V_{obs}
10/10/88	21:26:14	94	0.003	0.008	2.667	50.0	45.5
10/11/88	21:14:22	734	0.012	0.018	1.500	50.0	23.4
10/12/88	21: 3:17	397	0.016	0.020	1.250	50.0	19.5
10/20/88	21:17: 9	129	0.012	0.022	1.833	50.0	28.6
10/21/88	21: 5: 6	134	0.012	0.021	1.750	50.0	23.4
10/30/88	21: 7: 7	104	0.001	0.006	6.000	50.0	39.0
6/25/89	18:51:45	29	0.198	0.047	0.237	22.6	31.2
6/30/89	19:40:44	5	0.176	0.037	0.210	28.0	26.0
7/ 2/89	19:20: 2	57	0.275	0.034	0.124	14.8	26.0
7/ 4/89	18:59: 7	69	0.283	0.080	0.283	14.3	13.0
7/11/89	19:27:50	6	0.373	0.035	0.094	10.3	15.6
7/30/89	19:32: 6	13	0.267	0.028	0.105	15.4	13.0
8/ 2/89	19: 0:43	98	0.147	0.028	0.190	41.1	26.0
8/ 9/89	19:29: 0	221	0.071	0.023	0.324	50.0	32.5
8/10/89	19:18:39	143	0.054	0.022	0.407	50.0	32.5
8/27/89	19:43:50	1	0.040	0.000	0.000	50.0	15.6
9/ 1/89	18:51: 6	260	0.172	0.036	0.209	29.3	19.5
9/ 7/89	19:29:26	206	0.038	0.020	0.526	50.0	19.5
9/ 8/89	19:18:51	401	0.023	0.020	0.870	50.0	36.4
9/10/89	18:57:50	312	0.049	0.024	0.490	50.0	32.5
9/11/89	18:47:16	34	0.104	0.027	0.260	50.0	39.0
9/16/89	19:36:54	58	0.038	0.012	0.316	50.0	26.0
9/18/89	19:15:13	509	0.008	0.013	1.625	50.0	19.5
9/20/89	18:54:11	475	0.013	0.020	1.538	50.0	26.0
9/26/89	19:33: 9	47	0.014	0.019	1.357	50.0	24.7
9/27/89	19:22:48	15	0.067	0.016	0.239	50.0	22.1
10/ 5/89	19:39: 1	61	0.010	0.015	1.500	50.0	32.5
10/ 6/89	19:28:21	109	0.008	0.018	2.250	50.0	26.0
10/ 7/89	19:17:53	246	0.026	0.018	0.692	50.0	26.0
10/15/89	19:34:50	122	0.007	0.011	1.571	50.0	26.0
10/16/89	19:24:16	292	0.005	0.011	2.200	50.0	26.0
10/17/89	19:13:41	452	0.008	0.013	1.625	50.0	22.1
10/18/89	19: 3: 7	731	0.014	0.021	1.500	50.0	29.9
10/24/89	19:40:55	7	0.001	0.002	2.000	50.0	26.0
10/25/89	19:30:21	40	0.022	0.017	0.773	50.0	23.4
10/26/89	19:20: 0	132	0.007	0.013	1.857	50.0	28.6
10/27/89	19: 9:13	414	0.007	0.016	2.286	50.0	28.6
10/28/89	18:58:38	601	0.008	0.023	2.875	50.0	26.0
11/ 5/89	19:15:11	420	0.016	0.021	1.313	50.0	32.5
11/ 6/89	19: 4:37	635	0.012	0.024	2.000	50.0	13.0

Table C-4. (cont.)

DATE	TIME (GMT)	N_{obs}	$\overline{\tau}$	σ	ϵ	V_{inf}	V_{obs}
11/ 8/89	18:43:36	101	0.004	0.011	2.750	50.0	36.4
11/12/89	19:42:50	45	0.010	0.011	1.100	50.0	32.5
11/14/89	19:20:57	311	0.008	0.015	1.875	50.0	28.6
11/16/89	18:59:42	552	0.012	0.024	2.000	50.0	28.6
11/22/89	19:37:17	95	0.009	0.015	1.667	50.0	26.0
11/25/89	19: 5:55	43	0.016	0.022	1.375	50.0	26.0
11/26/89	18:55:34	2	0.000	0.000	-	50.0	23.4
12/ 6/89	18:49: 2	172	0.006	0.014	2.333	50.0	32.5
12/10/89	19:47:38	35	0.013	0.014	1.077	50.0	39.0
12/12/89	19:26:18	215	0.010	0.021	2.100	50.0	28.6
12/13/89	19:15:37	413	0.011	0.020	1.818	50.0	26.0
12/16/89	18:44: 8	21	0.012	0.014	1.167	50.0	26.0
12/20/89	19:41:59	115	0.009	0.015	1.667	50.0	26.0
12/21/89	19:31:12	276	0.002	0.010	5.000	50.0	28.6
12/22/89	19:20:31	285	0.012	0.020	1.667	50.0	28.6
12/24/89	18:58:58	182	0.010	0.024	2.400	50.0	28.6
12/30/89	19:36: 0	143	0.009	0.017	1.889	50.0	36.4
1/ 1/90	19:15:28	191	0.002	0.007	3.500	50.0	36.4
1/ 2/90	19: 3:50	695	0.008	0.018	2.250	50.0	26.0
1/ 8/90	19:40:34	104	0.020	0.017	0.850	50.0	26.0
1/10/90	19:19: 6	398	0.009	0.017	1.889	50.0	36.4
1/11/90	19: 8:25	525	0.015	0.021	1.400	50.0	28.6
2/ 1/90	18:45:48	8	0.094	0.020	0.213	50.0	32.5
2/ 5/90	19:42:54	122	0.015	0.016	1.067	50.0	32.5
2/14/90	19:47: 4	31	0.046	0.019	0.413	50.0	19.5
2/17/90	19:14:43	325	0.071	0.024	0.338	50.0	28.6
2/26/90	19:18:40	1102	0.032	0.024	0.750	50.0	28.6

Table C-5. Daily Comparisons of Inferred and Observed Meteorological Ranges for San Juan, Puerto Rico

DATE	TIME (GMT)	N_{obs}	$\overline{\tau}$	σ	ϵ	V_{inf}	V_{obs}
10/ 6/88	20:27:52	240	0.027	0.022	0.815	50.0	31.2
10/ 7/88	20:16:53	58	0.022	0.021	0.955	50.0	31.2
10/16/88	20:18:48	34	0.023	0.018	0.783	50.0	27.2
10/23/88	20:43:20	25	0.007	0.019	2.714	50.0	43.6
10/24/88	20:31:55	238	0.004	0.012	3.000	50.0	45.5
6/26/89	18:40:40	1	0.446	0.000	0.000	8.2	12.5
6/27/89	18:30:19	32	0.465	0.082	0.176	7.8	12.5
6/29/89	18: 9:24	105	0.143	0.040	0.280	43.9	41.6
7/ 4/89	18:59: 2	3	0.169	0.021	0.124	30.3	36.4
7/ 5/89	18:49:39	5	0.124	0.016	0.129	50.0	12.5
7/ 7/89	18:27:32	30	0.152	0.050	0.329	38.0	7.3
7/ 8/89	18:17:12	3	0.413	0.025	0.061	9.1	20.8
7/ 9/89	18: 6:57	1	0.582	0.000	0.000	6.0	20.8
7/16/89	18:35:14	76	0.121	0.038	0.314	50.0	36.4
7/18/89	18:14:12	140	0.125	0.039	0.312	50.0	31.2
7/25/89	18:43: 8	9	0.150	0.034	0.227	39.2	31.2
7/26/89	18:32:40	2	0.199	0.010	0.050	22.5	23.9
7/28/89	18:11:13	18	0.446	0.043	0.096	8.2	12.5
8/ 2/89	19: 0:32	1	0.214	0.000	0.000	20.4	15.6
8/ 3/89	18:49:58	66	0.159	0.038	0.239	34.4	28.1
8/ 4/89	18:39:43	49	0.122	0.036	0.295	50.0	29.1
8/ 6/89	18:18:41	153	0.160	0.045	0.281	34.0	31.2
8/ 7/89	18: 8:20	38	0.136	0.024	0.176	50.0	31.2
8/13/89	18:46:58	28	0.131	0.038	0.290	50.0	22.9
8/22/89	18:54: 7	54	0.050	0.024	0.480	50.0	31.2
8/24/89	18:33: 5	303	0.096	0.025	0.260	50.0	31.2
8/31/89	19: 1:36	21	0.080	0.018	0.225	50.0	31.2
9/ 1/89	18:50:55	39	0.061	0.019	0.311	50.0	31.2
9/ 2/89	18:40:15	112	0.047	0.018	0.383	50.0	31.2
9/ 4/89	18:19: 7	121	0.248	0.050	0.202	16.9	20.8
9/ 5/89	18: 8:39	84	0.214	0.036	0.168	20.4	16.6
9/10/89	18:57:51	8	0.064	0.020	0.313	50.0	31.2
9/12/89	18:36:43	4	0.121	0.033	0.273	50.0	29.1
9/15/89	18: 6: 5	8	0.127	0.034	0.268	50.0	31.2
9/21/89	18:43:46	9	0.065	0.018	0.277	50.0	26.0
9/29/89	19: 1:48	5	0.001	0.002	2.000	50.0	41.3
9/30/89	18:49:57	48	0.030	0.023	0.767	50.0	31.2
10/ 3/89	18:18:27	322	0.006	0.018	3.000	50.0	43.6
10/ 9/89	18:56:34	33	0.025	0.022	0.880	50.0	41.6
10/11/89	18:35:24	117	0.029	0.023	0.793	50.0	41.6

Table C-5. (cont.)

DATE	TIME (GMT)	N_{obs}	$\overline{\tau}$	σ	ϵ	V_{inf}	V_{obs}
10/18/89	19: 2:57	14	0.020	0.016	0.800	50.0	31.2
10/19/89	18:52:23	78	0.017	0.015	0.882	50.0	31.2
10/20/89	18:41:36	231	0.001	0.006	6.000	50.0	31.2
10/21/89	18:31: 8	344	0.002	0.010	5.000	50.0	23.4
10/22/89	18:20:33	481	0.003	0.013	4.333	50.0	29.1
10/23/89	18: 9:53	320	0.002	0.008	4.000	50.0	27.2
10/30/89	18:38:30	4	0.000	0.000	-	50.0	24.8
11/ 6/89	19: 4:20	24	0.004	0.010	2.500	50.0	31.2
11/ 7/89	18:53:40	61	0.016	0.022	1.375	50.0	31.2
11/ 8/89	18:43: 5	97	0.019	0.018	0.947	50.0	29.1
11/10/89	18:21:56	391	0.010	0.019	1.900	50.0	31.2
11/12/89	18: 1:40	6	0.096	0.016	0.167	50.0	27.0
11/16/89	18:59:38	38	0.009	0.015	1.667	50.0	31.2
11/17/89	18:48:51	70	0.011	0.018	1.636	50.0	31.2
11/18/89	18:38:11	143	0.024	0.023	0.958	50.0	31.2
11/20/89	18:16:56	311	0.018	0.023	1.278	50.0	29.1
11/21/89	18: 6:16	119	0.001	0.006	6.000	50.0	36.4
11/25/89	19: 4:58	7	0.031	0.013	0.419	50.0	31.2
11/26/89	18:54:18	56	0.013	0.016	1.231	50.0	43.6
11/27/89	18:43:31	82	0.014	0.022	1.571	50.0	37.0
11/28/89	18:32:56	140	0.013	0.021	1.615	50.0	43.6
12/ 5/89	18:59:25	54	0.002	0.006	3.000	50.0	43.6
12/ 6/89	18:48:45	170	0.003	0.008	2.667	50.0	43.6
12/ 7/89	18:38:11	470	0.007	0.017	2.429	50.0	41.6
12/ 8/89	18:27:29	354	0.004	0.010	2.500	50.0	41.6
12/ 9/89	18:16:43	428	0.001	0.006	6.000	50.0	43.6
12/10/89	18: 5:56	78	0.002	0.008	4.000	50.0	43.6
12/14/89	19: 4:33	47	0.025	0.020	0.800	50.0	39.0
12/15/89	18:53:52	95	0.002	0.010	5.000	50.0	40.3
12/16/89	18:43:12	213	0.003	0.012	4.000	50.0	40.3
12/17/89	18:32:25	402	0.002	0.009	4.500	50.0	36.3
12/18/89	18:21:56	392	0.001	0.006	6.000	50.0	31.2
12/19/89	18:10:57	204	0.001	0.004	4.000	50.0	31.2
12/23/89	19: 9:40	2	0.016	0.022	1.375	50.0	40.3
12/24/89	18:58:53	53	0.028	0.023	0.821	50.0	40.3
12/26/89	18:37:19	196	0.013	0.021	1.615	50.0	41.6
12/27/89	18:26:51	387	0.011	0.022	2.000	50.0	41.6
12/28/89	18:15:52	355	0.004	0.012	3.000	50.0	31.2
12/29/89	18: 5:31	26	0.023	0.016	0.696	50.0	31.2
1/ 2/90	19: 3:33	11	0.049	0.017	0.347	50.0	31.2

Table C-5. (cont.)

DATE	TIME (GMT)	N_{obs}	$\overline{\tau}$	σ	ϵ	V_{inf}	V_{obs}
1/ 3/90	18:52:46	85	0.025	0.021	0.840	50.0	31.2
1/ 5/90	18:31:18	712	0.010	0.020	2.000	50.0	41.6
1/ 6/90	18:20:31	327	0.004	0.013	3.250	50.0	41.6
1/ 7/90	18: 9:45	170	0.007	0.015	2.143	50.0	41.6
1/12/90	18:58: 6	15	0.007	0.020	2.857	50.0	31.2
1/13/90	18:46:54	91	0.013	0.020	1.538	50.0	36.4
1/14/90	18:35:47	178	0.019	0.022	1.158	50.0	31.2
1/21/90	19: 1:57	7	0.033	0.017	0.515	50.0	31.2
1/22/90	18:51: 4	242	0.017	0.018	1.059	50.0	31.2
1/25/90	18:18:49	158	0.214	0.060	0.280	17.1	20.8
1/26/90	18: 8:28	14	0.124	0.038	0.306	36.4	20.8
2/ 1/90	18:44:27	111	0.029	0.023	0.793	50.0	41.6
2/10/90	18:48:36	156	0.004	0.015	3.750	50.0	41.6
2/14/90	18: 6:33	2	0.292	0.025	0.086	12.2	27.4
2/18/90	19: 3:33	48	0.047	0.021	0.447	50.0	31.2
2/19/90	18:52:46	52	0.060	0.021	0.350	50.0	31.2
2/20/90	18:41:59	228	0.048	0.023	0.479	50.0	31.2
2/23/90	18:10:36	2	0.294	0.047	0.160	12.1	31.2
2/27/90	19: 7:49	24	0.035	0.015	0.429	50.0	31.2

Table C-6. Daily Comparisons of Inferred and Observed Meteorological Ranges for Tahiti Island

DATE	TIME (GMT)	N_{obs}	$\overline{\tau}$	σ	ϵ	V_{inf}	V_{obs}
10/ 2/88	2:19:27	52	0.023	0.018	0.783	50.0	19.5
10/ 3/88	2: 8:34	54	0.036	0.022	0.611	50.0	39.0
10/10/88	2:32:35	7	0.013	0.011	0.846	50.0	39.0
10/11/88	2:21:47	84	0.013	0.016	1.231	50.0	39.0
10/12/88	2:10:29	73	0.008	0.014	1.750	50.0	39.0
10/20/88	2:23:36	2	0.000	0.000	-	50.0	39.0
10/21/88	2:12:37	85	0.003	0.009	3.000	50.0	39.0
10/22/88	2: 1:50	1	0.068	0.000	0.000	50.0	39.0
10/29/88	2:25:26	11	0.005	0.007	1.400	50.0	32.5
10/31/88	2: 3:39	3	0.000	0.000	-	50.0	32.5
6/21/89	0:40:28	2	0.000	0.000	-	50.0	39.0
6/22/89	0:29:16	28	0.000	0.000	-	50.0	39.0
6/23/89	0:18:55	63	0.000	0.001	-	50.0	45.5
6/30/89	0:47:18	1	0.000	0.000	-	50.0	32.5
7/ 1/89	0:37:10	18	0.010	0.020	2.000	50.0	39.0
7/ 2/89	0:26:36	49	0.004	0.010	2.500	50.0	26.0
7/ 3/89	0:16:14	70	0.003	0.010	3.333	50.0	39.0
7/10/89	0:44:44	2	0.000	0.000	-	50.0	39.0
7/14/89	0: 3: 6	93	0.013	0.022	1.692	50.0	39.0
7/15/89	23:42:24	3	0.000	0.000	-	50.0	39.0
7/30/89	0:38:46	20	0.005	0.013	2.600	50.0	39.0
8/ 3/89	23:46:40	23	0.003	0.007	2.333	50.0	39.0
8/ 9/89	0:35:40	16	0.007	0.014	2.000	50.0	39.0
8/11/89	0:14:57	41	0.008	0.019	2.375	50.0	32.5
8/19/89	0:32:34	35	0.010	0.014	1.400	50.0	45.5
8/20/89	0:22:14	18	0.007	0.013	1.857	50.0	26.0
8/21/89	0:11:39	52	0.009	0.019	2.111	50.0	39.0
8/28/89	0:39:50	3	0.029	0.006	0.207	50.0	32.5
8/29/89	0:29:10	38	0.007	0.012	1.714	50.0	26.0
8/30/89	0:18:42	77	0.009	0.017	1.889	50.0	45.5
9/11/89	23:44:13	1	0.237	0.000	0.000	17.9	39.0
9/18/89	0:22: 0	74	0.002	0.010	5.000	50.0	52.0
9/19/89	0:11:39	80	0.006	0.014	2.333	50.0	39.0
9/25/89	0:49:45	1	0.010	0.000	0.000	50.0	45.5
9/26/89	0:39:17	17	0.016	0.018	1.125	50.0	39.0
9/27/89	0:28:37	39	0.023	0.020	0.870	50.0	32.5
9/28/89	0:18:29	21	0.039	0.020	0.513	50.0	39.0
10/ 5/89	0:45:35	4	0.000	0.000	-	50.0	19.5
10/ 6/89	0:35:14	37	0.012	0.015	1.250	50.0	52.0
10/ 7/89	0:24:46	57	0.008	0.012	1.500	50.0	39.0

Table C-6. (cont.)

DATE	TIME (GMT)	N_{obs}	$\overline{\tau}$	σ	ϵ	V_{inf}	V_{obs}
10/ 9/89	0: 3:44	157	0.009	0.019	2.111	50.0	32.5
10/15/89	0:41:30	8	0.024	0.014	0.583	50.0	45.5
10/16/89	0:31: 3	4	0.078	0.015	0.192	50.0	19.5
10/17/89	0:20:35	47	0.046	0.021	0.457	50.0	39.0
10/19/89	23:49: 5	4	0.227	0.017	0.075	16.0	19.5
10/24/89	0:48: 1	1	0.004	0.000	0.000	50.0	39.0
10/25/89	0:37: 1	15	0.009	0.018	2.000	50.0	39.0
10/26/89	0:26:40	49	0.012	0.013	1.083	50.0	39.0
10/27/89	0:16:18	68	0.013	0.018	1.385	50.0	39.0
11/ 4/89	0:32:45	9	0.024	0.019	0.792	50.0	26.0
11/ 5/89	0:22:11	27	0.015	0.020	1.333	50.0	52.0
11/ 7/89	0: 1:54	2	0.072	0.011	0.153	50.0	19.5
11/ 8/88	23:53:59	106	0.000	0.000	-	50.0	10.4
11/ 9/88	23:44: 9	73	0.001	0.006	6.000	50.0	10.4
11/15/89	0:17:16	1	0.095	0.000	0.000	50.0	45.5
11/23/89	0:33:23	48	0.000	0.000	-	50.0	52.0
12/ 5/89	23:56:59	2	0.207	0.000	0.000	17.8	11.7
12/10/89	0:54:25	1	0.000	0.000	-	50.0	13.0
12/11/89	0:43:58	2	0.017	0.000	0.000	50.0	32.5
12/12/89	0:33:10	35	0.030	0.023	0.767	50.0	19.5
12/13/89	0:22:37	11	0.043	0.013	0.302	50.0	39.0
12/14/89	0:11:55	53	0.037	0.023	0.622	50.0	39.0
12/21/89	0:37:59	2	0.064	0.006	0.094	50.0	32.5
12/23/89	0:16:50	18	0.010	0.022	2.200	50.0	39.0
12/24/89	23:55:49	2	0.137	0.013	0.095	30.7	19.5
12/29/89	0:53:40	3	0.000	0.000	-	50.0	39.0
12/31/89	0:32:33	15	0.016	0.012	0.750	50.0	39.0
1/ 8/90	0:47:33	7	0.022	0.022	1.000	50.0	39.0
1/ 9/90	0:36:53	42	0.017	0.015	0.882	50.0	39.0
1/10/90	0:26:12	66	0.011	0.014	1.273	50.0	45.5
1/11/90	0:15:25	110	0.017	0.019	1.118	50.0	45.5
1/18/90	0:42:32	1	0.086	0.000	0 000	50.0	32.5
1/19/90	0:30:55	3	0.047	0.009	0.191	50.0	26.0
1/20/90	0:21: 5	4	0.083	0.013	0.157	50.0	32.5
1/27/90	0:45:51	7	0.042	0.015	0.357	50.0	26.0
1/28/90	0:35: 4	11	0.041	0.023	0.561	50.0	39.0
1/29/90	0:24:24	36	0.023	0.015	0.652	50.0	26.0
1/30/90	0:13:30	32	0.034	0.022	0.647	50.0	26.0
2/24/90	0:47:20	8	0.047	0.017	0.362	50.0	19.5

Table C-7. Daily Comparisons of Inferred and Observed Meteorological Ranges for Ascension Island

DATE	TIME (GMT)	N_{obs}	$\overline{\tau}$	σ	ϵ	V_{inf}	V_{obs}
10/ 3/88	17:29:39	15	0.129	0.022	0.171	34.0	39.0
10/ 4/88	17:18:52	61	0.164	0.031	0.189	23.2	32.5
10/ 5/88	17: 7:52	107	0.165	0.047	0.285	23.0	52.0
10/ 6/88	16:56:40	88	0.143	0.042	0.294	28.6	78.0
10/12/88	17:32: 0	2	0.043	0.005	0.116	50.0	65.0
10/22/88	17:22:42	53	0.013	0.020	1.538	50.0	87.8
10/23/88	17:11:49	92	0.014	0.023	1.643	50.0	78.0
10/24/88	17: 0:30	16	0.020	0.022	1.100	50.0	32.5
10/31/88	17:24:50	13	0.044	0.020	0.455	50.0	52.0
11/ 1/88	17:13:50	62	0.010	0.016	1.600	50.0	55.3
6/24/89	15:30:17	9	0.003	0.004	1.333	50.0	97.5
6/29/89	14:38: 5	48	0.176	0.031	0.176	28.0	97.5
7/ 3/89	15:38: 4	1	0.063	0.000	0.000	50.0	52.0
7/ 8/89	14:45:52	133	0.185	0.047	0.254	25.5	97.5
7/ 9/89	14:35:31	23	0.230	0.046	0.200	18.6	78.0
7/13/89	15:34:59	4	0.000	0.000	-	50.0	78.0
7/26/89	15: 0:55	129	0.159	0.039	0.245	34.4	97.5
7/27/89	14:50:27	85	0.219	0.040	0.183	19.8	65.0
7/28/89	14:40:13	35	0.301	0.040	0.133	13.3	78.0
8/ 2/89	15:29:19	13	0.032	0.016	0.500	50.0	91.0
8/ 3/89	15:18:45	70	0.116	0.027	0.233	50.0	97.5
8/ 4/89	15: 8:17	93	0.148	0.049	0.331	40.4	78.0
8/ 6/89	14:47:28	113	0.140	0.040	0.286	46.3	78.0
8/ 7/89	14:37: 8	5	0.180	0.029	0.161	26.8	91.0
8/11/89	15:36:28	1	0.046	0.000	0.000	50.0	52.0
8/12/89	15:25:48	15	0.151	0.029	0.192	38.6	32.5
8/13/89	15:15:33	84	0.127	0.025	0.197	50.0	32.5
8/14/89	15: 5:11	124	0.100	0.028	0.280	50.0	52.0
8/16/89	14:44:10	60	0.207	0.041	0.198	21.3	78.0
8/21/89	15:33:16	5	0.085	0.025	0.294	50.0	2.3
8/22/89	15:22:49	32	0.080	0.022	0.275	50.0	6.5
8/24/89	15: 1:53	34	0.204	0.030	0.147	21.7	32.5
8/26/89	14:41:11	19	0.219	0.051	0.233	19.8	97.5
8/31/89	15:29:58	23	0.041	0.020	0.488	50.0	97.5
9/ 2/89	15: 8:56	95	0.032	0.022	0.688	50.0	26.0
9/ 9/89	15:36:41	4	0.145	0.014	0.097	42.5	78.0
9/11/89	15:15:52	76	0.105	0.023	0.219	50.0	65.0
9/19/89	15:33: 3	20	0.060	0.020	0.333	50.0	97.5
9/20/89	15:22:29	62	0.055	0.018	0.327	50.0	97.5
9/21/89	15:12: 1	75	0.094	0.027	0.287	50.0	10.4
9/22/89	15: 1:39	99	0.119	0.031	0.261	39.2	26.0

Table C-7. (cont.)

DATE	TIME (GMT)	N_{obs}	$\overline{\tau}$	σ	ϵ	V_{inf}	V_{obs}
9/23/89	14:50:59	23	0.270	0.048	0.178	13.3	18.2
9/24/89	14:40:51	6	0.265	0.026	0.098	13.5	20.8
9/29/89	15:29:25	11	0.084	0.024	0.286	50.0	97.5
10/ 8/89	15:35:56	4	0.037	0.012	0.324	50.0	65.0
10/10/89	15:14:35	96	0.151	0.025	0.166	26.3	65.0
10/13/89	14:42:58	18	0.148	0.048	0.324	27.1	65.0
10/17/89	15:41:53	1	0.000	0.000	-	50.0	97.5
10/20/89	15:10:23	109	0.041	0.022	0.537	50.0	97.5
10/27/89	15:37:30	5	0.036	0.023	0.639	50.0	87.8
10/28/89	15:27: 3	10	0.048	0.013	0.271	50.0	58.5
11/ 6/89	15:32:55	17	0.021	0.023	1.095	50.0	78.0
11/ 7/89	15:22:27	41	0.025	0.020	0.800	50.0	26.0
11/10/89	14:50:58	22	0.075	0.023	0.307	50.0	97.5
11/15/89	15:39:45	1	0.053	0.000	0.000	50.0	97.5
11/16/89	15:28: 7	4	0.040	0.023	0.575	50.0	39.0
11/20/89	14:45:31	28	0.106	0.033	0.311	49.0	65.0
11/25/89	15:33:40	25	0.040	0.020	0.500	50.0	97.5
12/ 5/89	15:28:26	39	0.022	0.016	0.727	50.0	97.5
12/ 6/89	15:17:26	49	0.025	0.016	0.640	50.0	78.0
12/ 7/89	15: 6:52	113	0.023	0.022	0.957	50.0	97.5
12/13/89	15:44: 1	5	0.006	0.004	0.667	50.0	97.5
12/14/89	15:33:21	17	0.030	0.017	0.567	50.0	97.5
12/23/89	15:38:15	14	0.025	0.012	0.480	50.0	78.0
12/24/89	15:27:28	18	0.011	0.016	1.455	50.0	97.5
12/25/89	15:17:33	29	0.043	0.024	0.558	50.0	91.0
12/28/89	14:45:12	13	0.011	0.013	1.182	50.0	97.5
1/ 1/90	15:43:52	1	0.007	0.000	0.000	50.0	45.5
1/ 2/90	15:32: 8	10	0.046	0.024	0.522	50.0	87.8
1/11/90	15:36:43	16	0.022	0.017	0.773	50.0	68.3
1/25/90	14:47:50	12	0.254	0.014	0.055	14.2	97.5
1/30/90	15:34:48	17	0.054	0.015	0.278	50.0	97.5
2/10/90	15:17:24	118	0.006	0.013	2.167	50.0	97.5
2/11/90	15: 6:37	167	0.013	0.020	1.538	50.0	97.5
2/17/90	15:43: 1	2	0.078	0.011	0.141	50.0	97.5
2/26/90	15:47:11	3	0.000	0.000	-	50.0	19.5